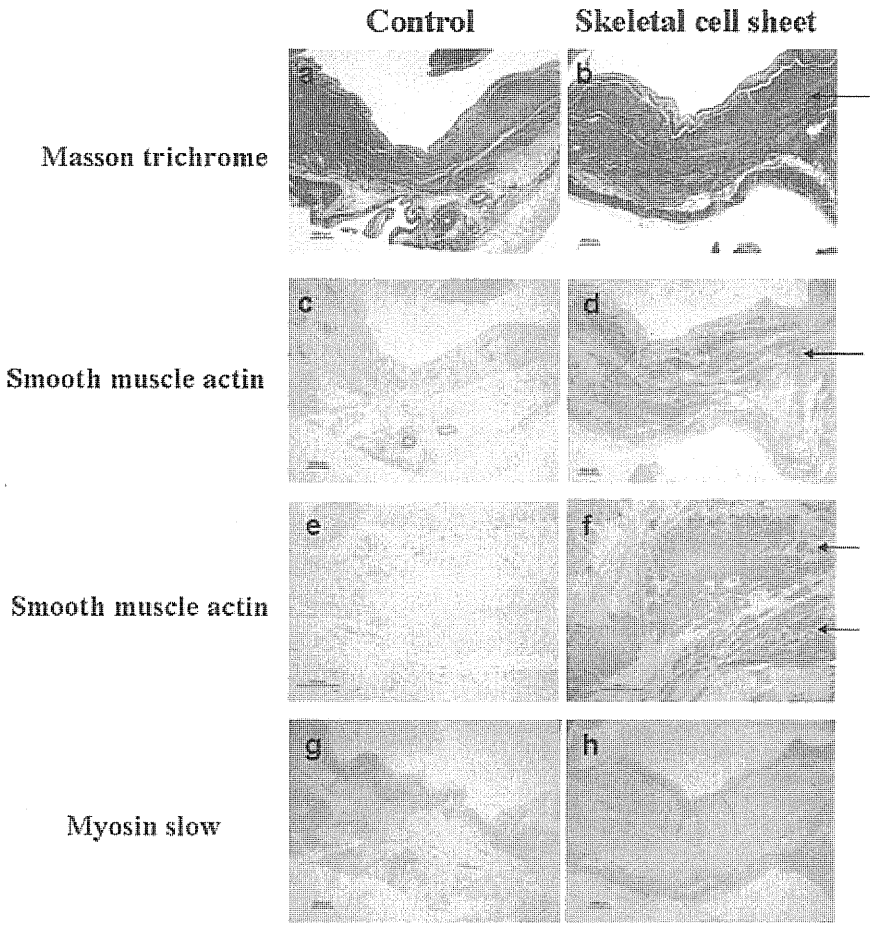

FIGURE 2. The detection of a large quantity of skeletal cells (SCs) in the center of the scar. (a and b) Masson trichrome staining reveals that some layered muscles are detected in the center of the scar in the SC sheet transplantation group, whereas not in the control. (c–f) Smooth muscle actin staining demonstrated that well-developed smooth muscle cells occupied in the center of the scar in the SC sheet transplantation group, whereas only smooth muscle cells which are formed vasculature are detected in the control. (g and h) Slow-type myosin staining showed that no positive cells exist in the center of the scar. This means that SCs which are detected in the center of the scar are not the residual myocyte after infarction.

RESULTS

Characteristics of Myoblast Sheet

We obtained monolayered myoblast sheets by lowering the temperature, which released them from the Poly(*N*-isopropylacrylamide)-grafted polystyrene. Its size is approximately 3 cm×2 cm^2 (Fig. 1a). H&E staining demonstrated that SC sheet contained a lot of SCs and SC sheets had an appearance of homogenous tissue, which thickness of one SC sheet was approximately 100 μm (Fig. 1b). Some smooth muscle cells are detected in the SC sheets, but those cells are not majority (Fig. 1c).

Histological Assessment

H&E staining demonstrated that transplanted SC sheets were attached in the epicardium (Fig. 1d) and oval-shaped cell that showed positive for eosin in cytoplasm were detected in the SC group microscopically in some layers over epicardium (Fig. 1e). Elastica Masson-Goldner showed that oval-shaped cells that supposed to origin from skeletal tissue exist in the transplantation site (Fig. 1f). These cells were not seen in the control group. And the SC group demonstrated decrease in the cross-sectional LV area compared with the C groups (Fig. 2a). Masson's trichrome staining showed that clustered SCs were detected in the center of the scar, whereas clustered SCs were not detected in the C group (Fig. 2a, b). Many clusters of well-developed smooth muscle cells exist in the center of the whole scar in the SC group, whereas in the C group, smooth muscle cells which formed vasculature exist in the scar (Fig. 2c–f). Although slow-type myosin-positive cells exist only on the endocardium and epicardium, those cells were not detected in the center of scar (Fig. 2g,h). So these figures depict that the skeletal muscle cells that exist in the center of the scar is not residual myocyte after infarction.

Quantification of Histopathology

In the SC group, vascular density was found to be significantly higher than in the C groups (SC vs. C=217.1±30.2 vs. 114.2±18.2 /field; $P<0.05$) (Fig. 3b).

Picro-sirius red staining demonstrated that % fibrosis was significantly reduced in the SC group compared with the C group (SC vs. C=1.6±0.2 vs. 3.1±0.3%; $P<0.05$) (Fig. 3b). Periodic acid-Schiff staining showed that cell diameter was significantly shorter in the SC group than the C group (SC vs. C=10.7±0.3 vs. 18.3±1.4 μm; $P<0.05$) (Fig. 3b).

These histological findings were universally identified in the native myocardial tissue without distinction of distance from the grafted region.

Functional Assessment of the Infarcted Myocardium

The FAS and LV end-ESA scores at baseline were not significantly different between the two groups.

Three months after the implantation, two-dimensional echocardiography showed significant improvement of the

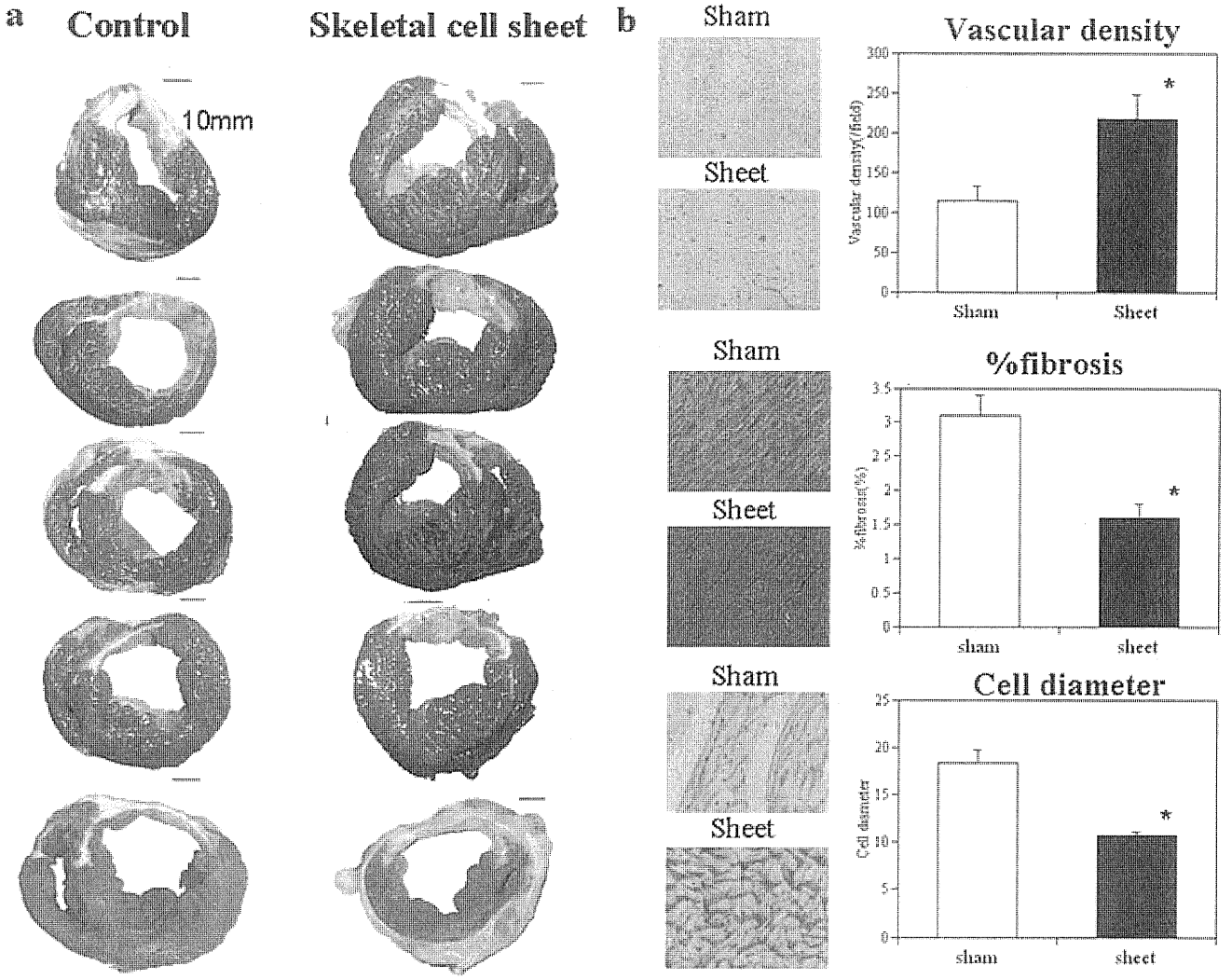

FIGURE 3. Macroscopic images of impaired myocardium receiving skeletal cell (SC) sheets and histological evaluation. (a) In the SC group, the anterior wall has recovered compared with the C group. In the SC group, the short axis area of the left ventricle (LV) is small compared with the C groups. In contrast, the C group shows a dilated LV and the anterior wall is thinner than in the SC groups. (b) Histological evaluation. Vascular density: the SC group showed a significant improvement in vascular density as assessed by immunostaining for the factor VIII-related antigen. *P less than 0.05 vs. C. The ratio of fibrosis-occupied area (% fibrosis) at a site remote from the infarcted heart region: picro-sirius red staining demonstrated that % fibrosis at a site remote from the infarcted heart region was significantly reduced in the SC group compared with the C group. *P less than 0.05 vs. C. The diameter of cardiomyocyte: the diameter of cardiomyocyte is significantly shorter in the SC group than the C group. *P less than 0.05 vs. C.

FIGURE 4. Global functional effects of infarcted myocardium receiving the implant. Global systolic function assessed by the fractional area shortening (FAS) (a) was significantly improved in the skeletal cell (SC) group 3 months after transplantation, and these functional improvements were preserved 6 months after SC sheet implantation. (b) The end-systolic area (ESA) was significantly smaller in the SC group than in the C groups 3 and 6 months after implantation. *P less than 0.05 vs. C, ■: SC sheet, ●: control.

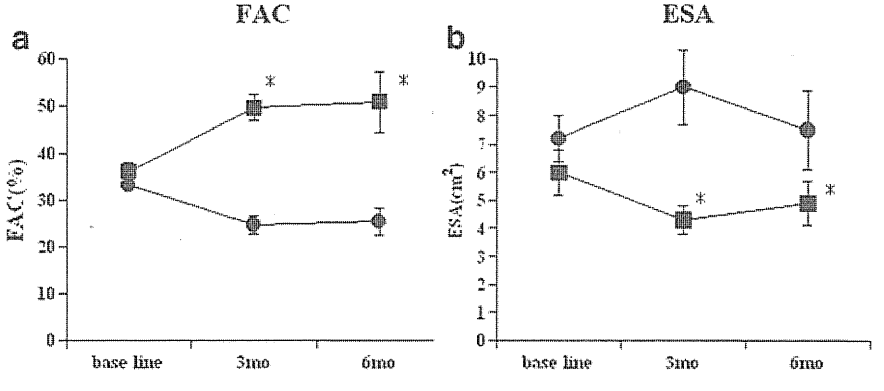

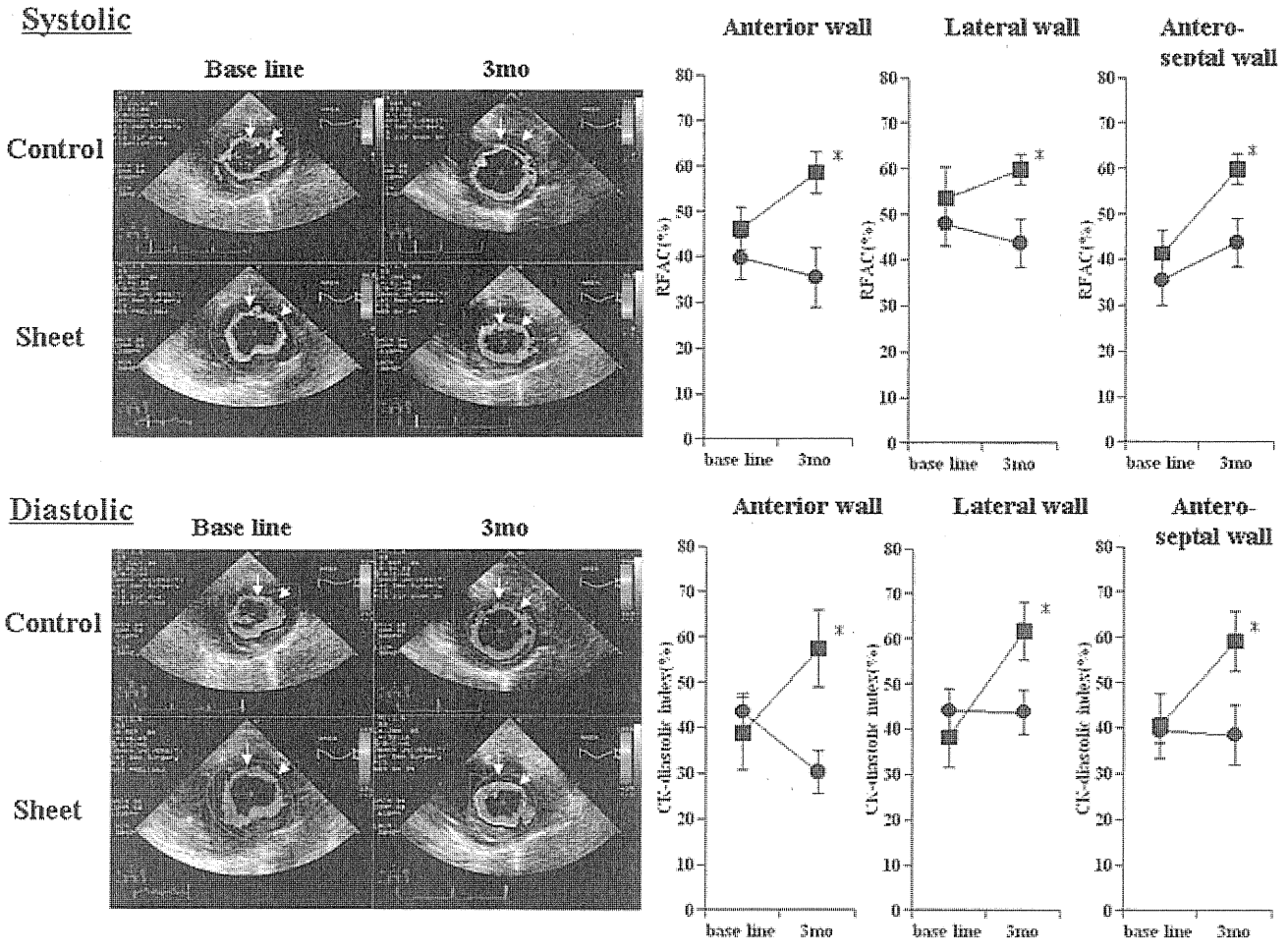

FIGURE 5. Systolic function: regional systolic function was significantly recovered in the skeletal cell (SC) group 3 months after implantation compared with the C group in the anterior, lateral, and anteroseptal wall. *P less than 0.05. Diastolic function: regional dysfunction was significantly recovered in the SC group 3 months after implantation compared with the C group in the anterior, lateral, and anteroseptal wall. Before treatment, diastolic dysfunction was observed in the infarction area of myocardium and the regional delayed relaxation was detected in the remote site of infarction by color kinesis. But this phenomenon was disappeared after SC sheet implantation. *P less than 0.05, ■: SC sheet, ●: control.

FAS (Fig. 4a) in the SC group compared with the C group (SC vs. C=49.5±2.8 vs. 24.6±2.0%, $P<0.05$). These functional improvements were preserved 6 months after implantation (SC vs. C=50.8±6.4 vs. 25.3±2.8%, $P<0.05$). The ESA was significantly smaller in the SC group than in the C group 3 months after the implantation (SC vs. C=4.3±0.5 vs. 9±1.3 cm^2, $P<0.05$) (Fig. 4b). These attenuation of LV dilatation were preserved 6 months after implantation (SC vs. C=4.9±0.8 vs. 7.5±1.4 cm^2, $P<0.05$). During this long-term observation, all SC sheet-treated animals were alive and exhibited no malignant arrhythmia assessed by 24-hour Holter ECG once a week (data not shown).

Before treatment, diastolic dysfunction was observed in the infarction area of myocardium and the regional delayed relaxation was detected in the remote site of infarction by color kinesis. After 3 months after implantation, CK-diastolic index in the lateral (SC vs. C=61.7±6.4 vs. 43.7±4.8%, $P<0.05$), anterior (SC vs. C=57.4±8.6 vs. 30.2±4.7%, $P<0.05$), and anteroseptal (SC vs. C=59±6.6 vs. 38.4±6.6%, $P<0.05$) segment were significantly ameliorated in the SC group compared with the C group, and regional systolic function in transplanted site was significantly improved in the SC group while not in the C groups (SC vs. C: lateral, 59.8±3.3 vs. 43.6±5.4%, $P<0.05$; anterior, 58.5±4.5 vs. 35.4±6.6%, $P<0.05$; anteroseptal, 59.8±3.3 vs. 43.6±5.4%, $P<0.05$), respectively (Fig. 5).

We could detect no ventricular premature beat for 24 hr by the Holter ECG in three myocardial infarction porcine received SC sheets.

Regional Myocardial Blood Flow and Residual Myocardial Tissue

PET study by using ^{15}0-water showed that the myocardial water-perfusable tissue fraction and myocardial blood flow were higher in the anterior wall where SC sheets were implanted compared with the myocardium receiving no sheets. These data depict that myocardial blood flow was better and microcirculation in the infarcted myocardium was preserved in the SC sheets implanted myocardium. PET study by using ^{18}F-FDG revealed that more viable myocardial tis-

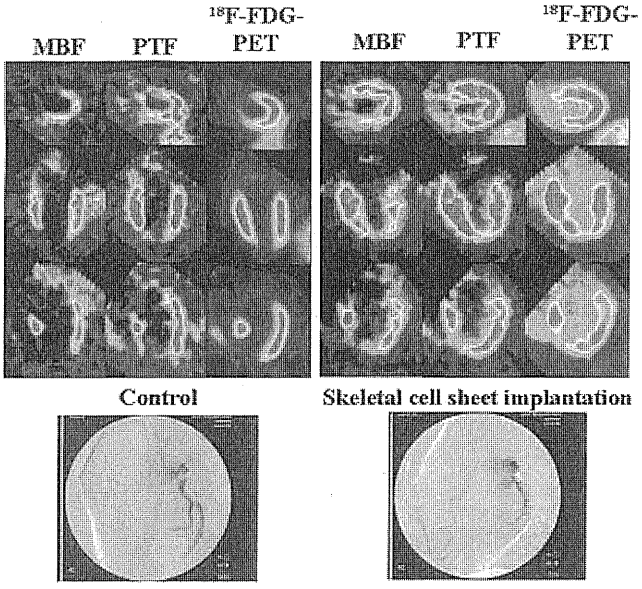

FIGURE 6. Positron emission tomography (PET) study revealed that perfusable tissue fraction (PTF) and myocardial blood flow (MBF) were higher and more viable myocardial tissues were preserved in the skeletal cell sheets implanted site compared with the myocardium receiving no sheets.

sues were preserved in the skeletal sheet implanted myocardium compared with the myocardium receiving no sheets. Coronary angiography revealed that LAD was occluded by the ameroid constrictor in both cases (Fig. 6).

DISCUSSION

Over the past several years, increasing awareness of the shortcomings of heart transplantation and left ventricular assist system implantation has led cardiovascular surgeons to consider alternative means of treating end-stage heart failure. In clinical setting, cellular cardiomyoplasty has been reported to have the potential of fundamental regenerative capability and has already been introduced in clinical trials with skeletal myoblast (*11*) or bone marrow mononuclear cells (*12*), and results suggest that it is a relatively feasible and safety therapy as a therapeutic angiogenesis. In this setting, cardiac tissue implantation was proposed to the treatment of end-staged heart failure as a new concept of regenerative therapy and experimentally some groups depicted it's effectiveness in the damaged myocardium (*13*, *14*). We also reported that cell sheets have great impacts on restoration of damaged myocardium in the rat infarction model (*3*, *4*) and dilated cardiomyopathy hamster (*5*). To convince the effectiveness of cell sheets in preclinical trial, we examined whether autologous SC sheets implantation might become one of the armamentarium of regenerative therapy for chronic heart failure caused by myocardial infarction in the porcine model.

The potential added advantages of the cell sheet implantation method include the implantation of a high number of cells with minimum cell loss. In contrast, the injection method is associated with a high loss of cells or surface proteins due to the trypsin treatment. Despite a high number of cell loss in needle injection, the cell sheet implantation method might provide the advantages of a higher number of cell implantation without cellular community destruction, leading the more improvement of cardiac performance rather than cell injection method (*4*). In case of needle injection, inflammation accompanied with destruction of myocardium induced by needle injection promotes graft death after cell transplantation (*15*).

To examine the effects of the SC sheet implantation therapy, we analyzed cardiac function and performed a histological assessment of the infarcted heart after SC sheet transplantation in a swine infarction model. SC sheet implantation therapy significantly induced angiogenesis, reduction of fibrosis histologically. And cell diameter of host myocyte was significantly attenuated its hypertrophy compared with the no treatment group. PET study revealed the better regional blood perfusion and better regional myocardial viability in the myocardium receiving cell sheets compared with the myocardium receiving no sheets.

Moreover, SC sheet implantation induced functional recovery of damaged myocardium. Especially, we demonstrated that the regional diastolic and systolic dysfunction was well recovered in the sheet implanted group. Before treatment, diastolic dysfunction of infarcted area and regional delayed relaxation of noninfarcted site were detected by color kinesis in the porcine infracted myocardium. After treatment, diastolic dysfunction of infarcted site was significantly recovered and the phenomenon of regional delayed relaxation in noninfarcted site was not seen. Presumably, implanted elastic myoblast sheets and a large quantity of well-developed smooth muscle cells, which are detected in the center of the scar, improved the regional diastolic dysfunction of implanted site. Although SC sheet can not contract in vivo after implantation, this recovery of diastolic disassociation of LV might result in the recovery of systolic dysfunction.

To the best of our knowledge, this is the first report in which tissue-engineered SC sheets implantation was successfully used to improve cardiac performance in a large animal model of ischemic myocardium according to the Laplace's theory.

The mechanisms of the restoration of damaged myocardium by SC sheet implantation might be complicated and many pathways might affect the recovery of ischemic myocardium. Recent reports depict that cell sheets enhance the recruitment of hematopoietic stem cells through the release of stromal-derived factor 1 (*4*). The fact of thicker anterior wall and the improvement of regional function might depend on both the recruitment of cytokine releasing stem cells, survival of grafted cells, and well-developed smooth muscle cells. And these cells might have good elasticity and these elastic cells and tissues softened the stiffness of anterior wall in association with the attenuating fibrosis even in the infarct area. This reduced stiffness of anterior wall might lead to the improvement of the diastolic dysfunction. Transplanted SCs cannot differentiate into cardiomyocyte anymore, but regional systolic function improved in the transplanted site. Probably, the improvement of regional diastolic function due to elastic cells might be responsible for the restoration of regional systolic dysfunction. Recent reports demonstrated that regional left ventricular myocardial relaxation was closely related to regional myocardial contraction (*16*) and the improvement of regional myocardial relaxation leads to the

recovery of global diastolic function (*17*). Moreover, the improvement of regional systolic function is closely related to global systolic function (*18*). We assume that this theory about the relationship between diastolic and systolic function is one of the mechanisms about the improvement of diastolic and systolic function in the cell sheet transplanted myocardium.

Question is why the well-developed smooth muscle cells exist in the center of the scar in the SC sheet group after transplantation despite a small quantity of smooth muscle cells in the SC sheet? Does a small quantity of smooth muscle cells in the SC sheet proliferate after transplantation? Do progenitor cells in the SC sheet differentiate to smooth muscle cells? Do progenitor cells or smooth muscle cells in the host myocardium migrate to the implanted site and proliferate? To the regret, there is no data to answer these questions exactly in this article and more detailed studies are needed to elucidate this important question.

Some reports depicted that the expression of hepatocyte growth factor (HGF) in the myoblast sheet transplanted ischemic myocardium is higher compared with the nontransplanted ischemic myocardium (*4*). HGF has an antifibrotic activity both through the activation of a matrix degradation pathway (*19*), restoration of cytoskeletal proteins on cardiomyocyte (*20*), and induce angiogenesis in the ischemic myocardium (*21*). Our study demonstrated that % fibrosis was significantly reduced in the SC sheet transplanted group. This paracrine secretion of HGF from SC sheets might attribute the reduction of % fibrosis. In our study, much more factor VIII-positive cells are detected in the SC sheet transplanted myocardium. This might be induced by paracrine secretion of HGF and angiogenesis might rescue the ischemic host cardiomyocyte and bring about the improvement of the distressed function of host cardiomyocyte. The distressed cytoskeletal proteins on the cardiomyocyte in the ischemic myocardium might be reorganized by the HGF secreted from skeletal sheet and the restoration of cytoskeletal proteins might lead to the improvement of cardiac function. And some reports demonstrated that myoblast sheets maintain the distressed cytoskeletal proteins on the host cardiomyocyte in the dilated cardiomyopathy hamster model (*5*). Consequently, cell sheet treatment is appropriate for recovery of ischemic cardiomyopathy. Recent research works demonstrated that several regenerative factors such as insulin-like growth factor-1 (*22*) and Thymosin b4 (*23*) were expressed in the rat ischemic myocardium model after myoblast sheet implantation by reverse-transcriptase polymerase chain reaction analysis (data not shown). After myoblast sheet transplantation to ischemic myocardium, several regenerative factors are expressed in the transplanted site, and these long-term and low-dosed expressed regenerative factors might cooperatively restore the damaged myocardium.

We could find no ventricular premature beat analyzed by Holter ECG after SC sheet implantation. We have already proved that in the rat infarction model, arrhythmia is less in the SC sheet implantation group compared with the needle injection group and this work represented that more monocyte chemotactic protein-1-positive cells and CD11b (macrophage marker)-positive cells were detected in the needle injection group compared with SC sheet implantation (data not shown). We speculate that needles destroy the myocardium and this destroyed myocardium may induce the inflammation and this inflammation may induce the arrhythmia. Conversely, SC sheet implantation technique normally doses not destroy the myocardium when they are implanted to recipient heart. Moreover, SC sheet will survive on the epicardium and electrical wave originated from implanted myoblasts may not deliver to the recipient myocardium directly. But when we implant myoblasts by needle injection, implanted myoblasts survive in the center of the myocardium and electrical wave will deliver to the myocardium directly, leading to the arrhythmia.

In conclusion, we have preclinically demonstrated SC sheets produced histologically and functionally apparent prevented the deterioration of the impaired myocardium in the swine model. These data provide a basis for attempting clinical cell sheet implantation in ischemic disease as the armamentarium to promote the regeneration of chronic heart failure caused by myocardial infarction.

ACKNOWLEDGMENTS

The authors thank Shigeru Matsumi and Masako Yokoyama for their excellent technical assistance.

REFERENCES

1. Shimizu T, Yamato M, Akutsu T, et al. Fabrication of pulsatile cardiac tissue grafts using a novel 3-dimensional cell sheet manipulation technique and temperature-responsive cell culture surfaces. *Circ Res* 2002; 90: e40.
2. Shimizu T, Sekine H, Isoi Y, et al. Long-term survival and growth of pulsatile myocardial tissue grafts engineered by the layering of cardiomyocyte sheets. *Tissue Eng* 2006; 12: 499.
3. Miyagawa S, Sawa Y, Sakakida S, et al. Tissue cardiomyoplasty using bioengineered contractile cardiomyocyte sheets to repair damaged myocardium: Their integration with recipient myocardium. *Transplantation* 2005; 80: 1586.
4. Memon IA, Sawa Y, Fukushima N, et al. Repair of impaired myocardium by means of implantation of engineered autologous myoblast sheets. *J Thorac Cardiovasc Surg* 2005; 130: 1333.
5. Kondoh H, Sawa Y, Miyagawa S, et al. Longer preservation of cardiac performance by sheet-shaped myoblast implantation in dilated cardiomyopathic hamsters. *Cardiovasc Res* 2006; 69: 466.
6. Hata H, Matsumiya G, Miyagawa S, et al. Grafted skeletal myoblast sheets attenuate myocardial remodeling in pacing-induced canine heart failure model. *J Thorac Cardiovasc Surg* 2006; 132: 918.
7. Mor-Avi V, Vignon P, Bales AC, et al. Acoustic quantification indexes of left ventricular size and function: Effects of signal averaging. *J Am Soc Echocardiogr* 1998; 11: 792.
8. Ishii K, Miwa K, Makita T, et al. Prolonged postischemic regional left ventricular delayed relaxation or diastolic asynchrony detected by color kinesis following coronary vasospasm. *Am J Cardiol* 2003; 91: 1366.
9. Fukui S, Kitagawa-Sakakida S, Kawamata S, et al. Therapeutic effect of midkine on cardiac remodeling in infarcted rat hearts. *Ann Thorac Surg* 2008; 85: 562.
10. Iida H, Yokoyama I, Agostini D, et al. Quantitative assessment of regional myocardial blood flow using oxygen-15-labelled water and positron emission tomography: A multicentre evaluation in Japan. *Eur J Nucl Med* 2000; 27: 192.
11. Dib N, Michler RE, Pagani FD, et al. Safety and feasibility of autologous myoblast transplantation in patients with ischemic cardiomyopathy: Four-year follow-up. *Circulation* 2005; 112: 1748.
12. Perin EC, Dohmann HF, Borojevic R, et al. Transendocardial, autologous bone marrow cell transplantation for severe, chronic ischemic heart failure. *Circulation* 2003; 107: 2294.
13. Leor J, Aboulafia-Etzion S, Dar A, et al. Bioengineered cardiac grafts. A new approach to repair the infarcted myocardium? *Circulation* 2000; 102(suppl III): III-56.

14. Li RK, Jia ZQ, Weisel RD, et al. Survival and function of bioengineered cardiac grafts. *Circulation* 1999; 100(suppl II): II-63.
15. Suzuki K, Murtuza B, Beauchamp JR, et al. Role of interleukin-1beta in acute inflammation and graft death after cell transplantation to the heart. *Circulation* 2004; 110(11 suppl 1): II-219.
16. Tanaka H, Kawai H, Tatsumi K, et al. Relationship between regional and global left ventricular systolic and diastolic function in patients with coronary artery disease assessed by strain rate imaging. *Circ J* 2007; 71: 517.
17. Tanaka H, Kawai H, Tatsumi K, et al. Improved regional myocardial diastolic function assessed by strain rate imaging in patients with coronary artery disease undergoing percutaneous coronary intervention. *J Am Soc Echocardiogr* 2006; 19: 756.
18. Moller JE, Hillis GS, Oh JK, et al. Wall motion score index and ejection fraction for risk stratification after acute myocardial infarction. *Am Heart J* 2006; 151: 419.
19. Liu Y, Rajur K, Tolbert E, et al. Endogenous hepatocyte growth factor ameliorates chronic renal injury by activating matrix degradation pathways. *Kidney Int* 2000; 58: 2028.
20. Miyagawa S, Sawa Y, Taketani S, et al. Myocardial regeneration therapy for heart failure: Hepatocyte growth factor enhances the effect of cellular cardiomyoplasty. *Circulation* 2002; 105: 2556.
21. Taniyama Y, Morishita R, Aoki M, et al. Therapeutic angiogenesis induced by human hepatocyte growth factor gene in rat and rabbit hindlimb ischemia models: Preclinical study for treatment of peripheral arterial disease. *Gene Ther* 2001; 8: 181.
22. Li Q, Li B, Wang X, et al. Overexpression of insulin-like growth factor-1 in mice protects from myocyte death after infarction, attenuating ventricular dilation, wall stress, and cardiac hypertrophy. *J Clin Invest* 1997; 100: 1991.
23. Bock-Marquette I, Saxena A, White MD, et al. Thymosin beta4 activates integrin-linked kinase and promotes cardiac cell migration, survival and cardiac repair. *Nature* 2004; 432: 466.

ELSEVIER

European Journal of Cardio-thoracic Surgery 38 (2010) 450–455

EUROPEAN JOURNAL OF CARDIO-THORACIC SURGERY

www.elsevier.com/locate/ejcts

Engineering a novel three-dimensional contractile myocardial patch with cell sheets and decellularised matrix☆,☆☆

Hiroki Hata[a,b,*], Antonia Bär[a], Suzanne Dorfman[a], Zlata Vukadinovic[a], Yoshiki Sawa[c], Axel Haverich[a,b], Andres Hilfiker[a]

[a] *Leibniz Research Laboratories for Biotechnology and Artificial Organs (LEBAO), Hannover Medical School, Hannover, Germany*
[b] *Department of Cardiac, Thoracic, Transplantation and Vascular Surgery, Hannover Medical School, Hannover, Germany*
[c] *Department of Cardiovascular Surgery, Osaka University Graduate School of Medicine, Suita, Japan*

Received 1 October 2009; received in revised form 30 January 2010; accepted 4 February 2010; Available online 23 March 2010

Abstract

Objectives: A persistent problem in generating a functional myocardial patch is maintaining contractions in a thicker construct. Thus far, we have successfully created contracting constructs with a defined directionality by seeding neonatal rat cardiomyocytes (CMs) on decellularised porcine small-intestinal submucosa (SIS). Here, we report our efforts in generating a thicker contracting construct by combining CM cell sheets with CM-seeded SIS. **Methods:** Porcine SIS was decellularised, opened along the longitudinal axis, fixed in a metal frame (45 mm × 25 mm) and seeded onto the submucosal side with neonatal rat CMs at a density of 1.8×10^5 cells cm^{-2}. CM sheets were prepared using temperature-responsive dishes by seeding CMs at a density of 4.0×10^5 cells cm^{-2}. Three days after CM seeding, one- or three-layered CMs sheet(s) were stacked onto seeded SIS. Construct contraction was observed for an additional 10 days followed by histological analysis. **Results:** Stacked CM sheets contracted spontaneously and synchronously with seeded SIS after adherence. A large portion of analysed constructs showed a defined contraction direction, parallel to the longitudinal axis (seeded SIS: 83%, seeded SIS + 1 sheet: 70%, seeded SIS + 3 layered sheets: 71%). This finding was in agreement to the histological finding of aligned CMs parallel to the longitudinal axis. The thickness of seeded SIS with and without three-layered sheets was approximately 800 μm and 500 μm, respectively. **Conclusions:** By combining layered CM sheets with CM-seeded SIS, a three-dimensional myocardial patch with contraction in a defined direction was successfully generated. This may represent an intermediate step to a multiple layered, vascularised contractile myocardial graft.

Keywords: Tissue engineering; Small-intestinal submucosa; Cell sheet; Myocardial patch

1. Introduction

A major aim of tissue engineering is the production of a functional three-dimensional structure, aimed to restore, support or supersede native tissue function. Thus far, multiple tissue-engineered constructs have been developed and clinically applied since the term 'tissue engineering' was first introduced in 1987 [1]. Above all, engineering of myocardial tissue may become a pressing need in an ageing society with increasing cardiovascular morbidity [2]. Although several reports of producing cardiac tissue have been made since the late 1950s, engineering a fully functional and transplantable heart muscle has not yet been achieved due to the structural and functional complexity of native heart muscle [1–3].

Research conducted by Zimmermann and Zhao [3,4] has suggested three potential approaches to construct functional contractile cardiac tissue: (1) seeding cardiomyocytes (CMs) on a synthetic or biological scaffold; (2) using soluble collagen and other extracellular matrix (ECM) components to entrap CMs; and (3) stacking CM sheets to form multilayered cardiac muscle constructs. With respect to approach (1), our laboratory has successfully developed a contracting artificial myocardial tissue by seeding CM on a collagen scaffold [5]. Progress in this direction was achieved through the replacement of the collagen scaffold with decellularised porcine small-intestinal submucosa (SIS) as the matrix. When seeded with neonatal rat CM, a contracting construct with a defined direction was generated [6].

Cell sheet technology (approach 3) has several advantages; for example, the preservation of cell-to-cell connec-

☆ Presented at the 23rd Annual Meeting of the European Association for Cardio-thoracic Surgery, Vienna, Austria, October 18–21, 2009.

☆☆ *Sources of funding*: This study was supported by the CORTISS Foundation. H.H. received a fellowship from the Japan Heart Foundation and the Uehara Memorial Foundation.

* Corresponding author. Address: Leibniz Research Laboratories for Biotechnology and Artificial Organs (LEBAO), Hannover Medical School, Carl-Neuberg-Strasse 1, D-30625 Hannover, Germany. Tel.: +49 511 532 8913; fax: +49 511 532 8819.
E-mail address: Hata.Hiroki@mh-hannover.de (H. Hata).

1010-7940/$ – see front matter
doi:10.1016/j.ejcts.2010.02.009

tion with ECM, the maintenance of electrophysiological and contractile performance, the feasibility of stacking multiple sheets and the independence from potentially immunogenic or pathogenic scaffold materials [1,7]. However, the maximum thickness and strength achievable, relative to native tissue, remains equivocal. Our laboratory has investigated the transfer of cell sheets of various origins, as a regenerative therapy option in different animal models [8,9] and in a clinical study in Osaka University.

Decellularised porcine SIS is an acellular ECM rich in collagen, glycosaminoglycans and growth factors, and been characterised as a complete absorbable biocompatible framework [10]. As a result of these characteristics, it has great potential for use in both *ex vivo* tissue engineering and in reconstructive surgery. SIS and similar ECM scaffolds, for example, decellularised porcine urinary bladder matrices have also been applied in animal models of cardiac repair [11,12].

Herein, we describe our next step towards an implantable myocardial patch combining our previous success with CM-seeded SIS and CM cell sheets.

2. Materials and methods

2.1. Animal care

This work was approved by the Institutional Review Board and the Institutional Animal Care and Use Committee protocols of Hannover Medical School. All animals received humane care in compliance with the European Convention on Animal Care.

2.2. Decellularisation of porcine SIS

Porcine small intestine was harvested from anaesthetised German Landrace pigs weighing 20–25 kg and cut into short segments. After mechanical removal of tunica mucosa and tunica serosa, segmented intestines were chemically decellularised using a modified method of Meezan et al. [13]. In brief, decellularisation was performed using 4% sodium-deoxycholate and 0.1% sodiumazide under continuous shaking at 4 °C for 2 h. SISs were washed with phosphate-buffered saline (PBS) containing 0.1% neomycin sulphate and 1% penicillin–streptomycin solution under continuous shaking for 7 days at 4 °C. Following the last wash, SISs were sterilised by 150 Gy gamma-ray irradiation for 75 min. Just before use, they were cut open along the longitudinal axis and fixed on a 45 mm × 25 mm metal frame.

2.3. Preparation of CM-seeded SIS and CM sheet

Neonatal rat CMs were isolated as described previously [14]. In brief, ventricles from 1- to 2-day-old Sprague Dawley rats were minced in ADS buffer (116 mM NaCl, 20 mM HEPES, 10 mM NaH_2PO_4, 5.4 mM KCl, 0.8 mM $MgSO_4$ and 5.6 mM glucose) and enzymatically digested with type II collagenase (Worthington, Lakewood, NJ, USA) and pancreatin (Sigma–Aldrich, St. Louis, MO, USA) at 37 °C. CMs were enriched in the primary CM isolates either by differential centrifugation through discontinuous Percoll gradient or with the preplating procedure. For preplating, CM isolates in culture medium were cultivated in flasks for 1 h. Following 1 h, the remaining supernatant in the flask contained an enriched CM fraction. Purification of CM by a discontinuous Percoll gradient was prepared as described before [15] using two density solutions, 1.062 and 1.082 g ml^{-1}, made from Percoll reagent (GE Healthcare). The collected cells after Percoll gradient centrifugation were seeded at a density of 1.8×10^5 cells cm^{-2} onto the submucosa side of SIS fixed in a metal frame. The SIS with cells were cultivated in 1:4 Dulbecco's Modified Eagle's Medium (Gibco, Invitrogen):medium 199 (PAA, Pasching, Austria), 10% foetal calf serum (PAA), 5% horse serum (Gibco) and 1% penicillin–streptomycin in a humidified 37 °C atmosphere with 5% CO_2.

For the generation of cell monolayer sheets, preplated CMs were cultivated in temperature-responsive dishes as described before [7]. In brief, CMs were seeded at a density of 4.0×10^6 cells per poly(N-isopropylacrylamide) grafted temperature-responsive dish (UpCell; Cellseed, Tokyo, Japan) with a diameter of 35 mm and incubated in culture medium for 3 days.

2.4. Transfer of CM sheet onto decellularised SIS

After 3 days of cultivation, CM cell sheets were detached through a temperature change from 37 °C to 20 °C for approximately 30 min. After detachment, one cell sheet ($n = 24$) or three-layered cell sheets ($n = 18$) were stacked onto a CM-seeded SIS according to previously described procedures [7]. Briefly, the entire CM sheet with media was gently aspirated and transferred onto the SIS. Media was then gently dropped onto the centre of the sheet to spread the folded parts. Excess media was aspirated to allow the cell sheet to adhere to the SIS. After 30 min and using the same protocol, additional CM sheets were transferred and spread onto the formerly attached cell sheet. Approximately 30 min were found to be sufficient for adhesion of the layered sheet(s). In addition, one CM sheet on an un-seeded SIS ($n = 13$) and CM-seeded SIS without CM sheet ($n = 12$) were prepared. All constructs were incubated at 37 °C for an additional 10 days and the culture medium was changed every 2 days.

2.5. Assessment of cell population

Cells after Percoll gradient or preplating were seeded on 10 temperature-responsive dishes (3.0×10^6 cells per dish), respectively, and incubated in a culture medium as described above for 1 day. After fixation with 4% formaldehyde, cells were stained with monoclonal anti-α-sarcomeric actinin (Sigma) or anti-prolyl-4β-hydroxylase (Acris, Hiddenhausen, Germany). Nuclei were counterstained with 4′,6-diamidino-2-phenylindole (DAPI) (Sigma). The images were photographed using an inverted research microscope (Axio Observer A1, Zeiss). Cell population percentages were calculated by dividing the number of respective cells by the total number of cells. Four randomly selected optical fields (0.083 mm^2) per dish were analysed and an image analysis software (ImageJ 1.40 g, Wayne Rasband, NIH, USA) was used.

2.6. Microscopic and macroscopic observation

All constructs were observed by means of an inverted optical microscope (CKX41, Olympus) to count the synchronous contraction rate and to observe the contraction direction. The contractile direction, within approximately 30° from the longitudinal axis of the SIS, was defined as an oriented contraction parallel to the longitudinal axis. The ratio of constructs showing oriented contractions was calculated by dividing the number of respective myocardial grafts by the total number of myocardial grafts. Microscopic images of contracting CM sheets on SIS were recorded using a motorised inverted research microscope (Axio Observer Z1, Zeiss). Macroscopic images of contracting myocardial patches were also recorded using a digital movie camera (DMX-HD2, SANYO).

2.7. Histological analysis

For assessment of collagen fibre alignment, a small piece of decellularised SIS was fixed with 4% paraformaldehyde and stained with anti-collagen I (Sigma) detected by Alexa Fluor 488 (Molecular Probes, Eugene). For characterisation of the seeded cells and cell sheets on SIS, samples were cut into approximately 4 cm^2 squares, fixed with 4% paraformaldehyde and stained with Alexa Fluor 488-conjugated phalloidin (Molecular Probes) or monoclonal anti-α-sarcomeric actinin and Alexa Fluor 488 (Molecular Probes). Cell nuclei were counterstained with DAPI. Additional samples were fixed with 10% formalin, embedded in paraffin, cut into 6-μm cross-sections, and stained with haematoxylin and eosin or monoclonal anti-connexin 43 (Sigma) and Alexa Fluor 488. Connexin 43-stained samples were counterstained with DAPI. Stained sections were analysed and documented using an inverted research microscope (Axio Observer A1).

2.8. Statistics

All data are presented as mean ± standard deviation.

3. Results

3.1. Decellularised SIS

Decellularised SIS was pliable, durable and easily stretched onto a metal frame (Fig. 1(A) and (B)). Collagen fibres in the decellularised SIS were oriented along the longitudinal axis (Fig. 1(C)).

3.2. Cell population after Percoll gradient and preplating

CMs and fibroblasts were identified through staining for α-sarcomeric actinin and prolyl-4β-hydroxylase, respectively. The cell suspension after Percoll gradient centrifugation contained 86.9 ± 3.8% CM and 10.5 ± 1.0% fibroblasts, while preplating isolates contained 74.6 ± 3.6% CM and 21.6 ± 5.6% fibroblasts.

SIS were seeded with both CM isolates; however, SIS seeded with preplated CM isolates resulted in a less synchronous contraction pattern and over a shorter duration than SIS seeded with the Percoll CM isolates (data not shown). Similarly, CM cell sheets were made with both CM isolates. Cell sheets and subsequent stacking made with Percoll CM isolates resulted in a less tight adhesion as shown by cross-section histological assessment (Fig. 2). Based on these data, CM from Percoll isolates were used as the cell source for direct seeding onto the SIS, and CM cell sheets stacked on the SIS were made with preplated CM isolates.

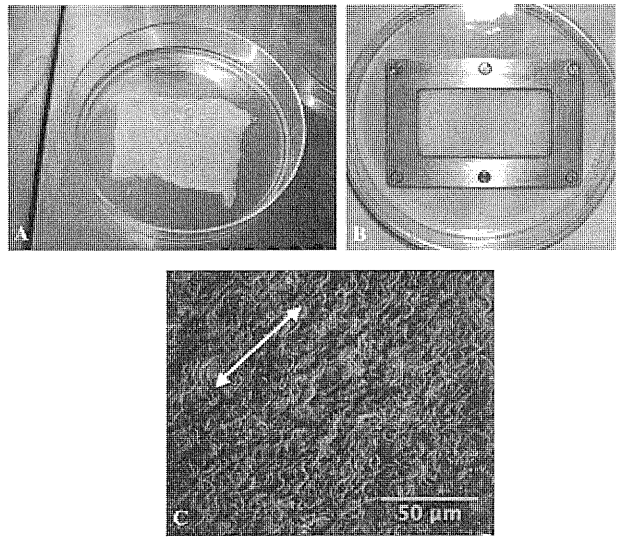

Fig. 1. Decellularised porcine small-intestinal submucosa (SIS) (A), fixed in a metal frame such that the long axis of the SIS was parallel to the long axis of the metal frame (B). Anti-collagen I staining revealed that collagen fibre in SIS aligned along the longitudinal axis (C). Scale bars: 50 μm.

3.3. Macroscopic and microscopic observation

All Percoll CM-seeded SIS started to contract spontaneously 1–2 days after initial CM seeding. After lowering culture temperature from 37 °C to 20 °C, CM cell sheets

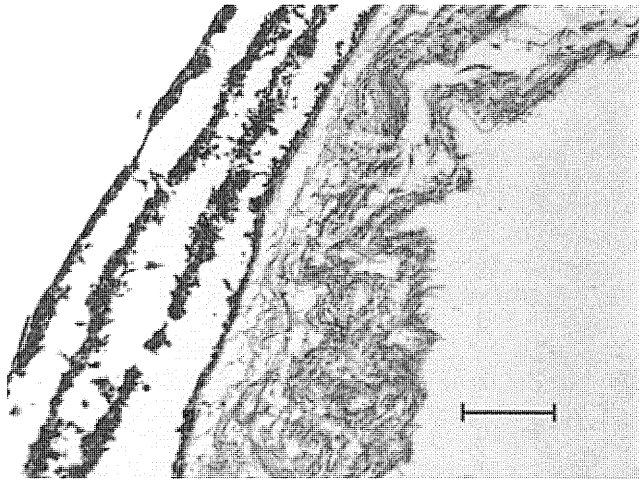

Fig. 2. Haematoxylin and eosin staining of a cross-sectional slice of a myocardial patch made with three-layered Percoll-enriched cardiomyocyte (CM) sheets on a CM-seeded small-intestinal submucosa (SIS). CM sheets did not adhere to one another or to the seeded SIS. Scale bars: 200 μm.

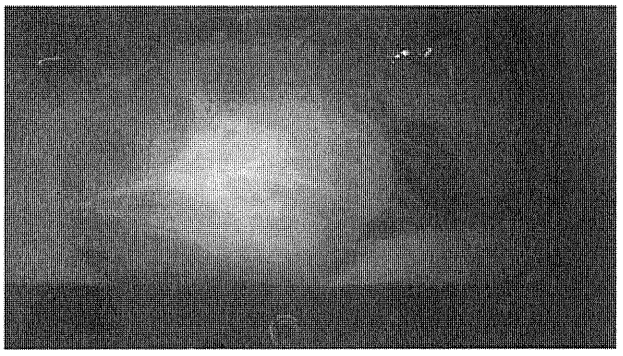

Fig. 3. Macroscopic appearance of seeded SIS with three-layered cardiomyocyte sheets.

spontaneously detached as a single unit maintaining contractility without enzymatic treatment. Initially, a transferred CM sheet shrank to some extent, and had asynchronous contractions in multiple directions. As shown in Fig. 3, the cell sheet could be manipulated to lie flat on either seeded or un-seeded SIS. After stacking, the cell sheets placed on SIS collectively contracted in a defined direction parallel to the longitudinal axis of the SIS (Supplemental Video 1). The wave-like contraction pattern was observed for both CM sheets layered on CM-seeded SIS and un-seeded SIS. All constructs, regardless of the number of cell sheets, began contracting a few minutes after transfer. Approximately 50% of all myocardial patches with one or three cell sheet(s) on CM-seeded SIS contracted until day 10 after sheet transplantation, while un-seeded SIS with one CM sheet contracted for only 4 days after cell sheet transfer. A large proportion of analysed constructs showed an oriented contraction parallel to the longitudinal axis of the SIS 3 days after cell sheet transfer; CM-seeded SIS without cell sheets: 83%, CM-seeded SIS with one CM sheet: 70%, CM-seeded SIS with three-layered CM sheets: 71%. Macroscopic observation of CM-seeded SIS with three-layered CM sheets with a defined contraction orientation and parallel to the longitudinal axis of SIS is shown in Supplemental Video 2.

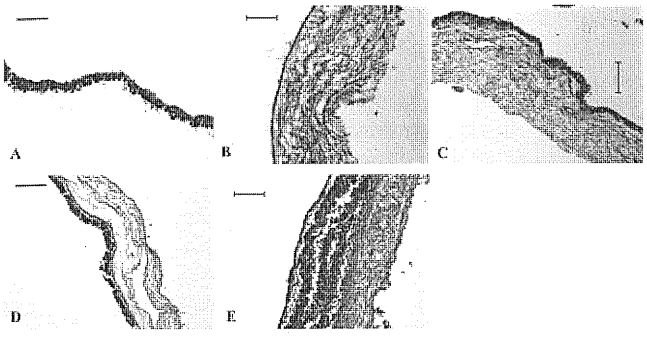

Fig. 4. Haematoxylin and eosin staining of cross-sectional slices of myocardial patches. Small-intestinal submucosa (SIS) was seeded with Percoll cardiomyocytes (CM), cell sheets were made with preplated CM. (A) single CM cell sheet; (B) decellularised porcine SIS; (C) CM-seeded SIS; (D) CM-seeded SIS with 1 CM sheet; (E) CM-seeded SIS with three-layered CM sheets. Scale bars: 100 μm (A), 200 μm (B–E).

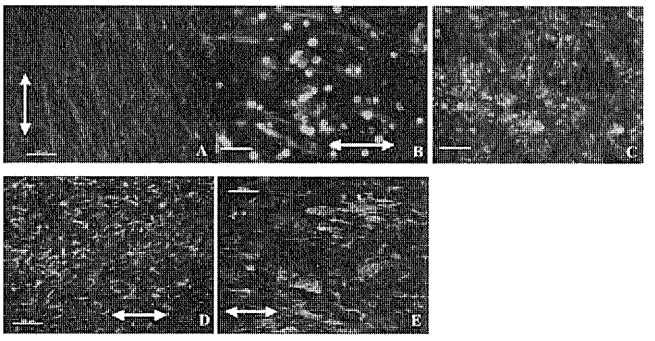

Fig. 5. Immunohistochemical assessment of decellularised small-intestinal submucosa (SIS) seeded with cardiomyocytes (CM) (A and B), CM sheet detached from the temperature-responsive dish (C), and CM sheet on seeded SIS (D and E). Cells were stained with phalloidin (A and C) or anti-α-sarcomeric actinin (B, D and E). Nuclei were stained with DAPI (A–E). Note orientation of CM cell sheet on seeded SIS (D and E) and seeded CM on SIS (A and B), which are consistent with the longitudinal axis of SIS indicated by white arrows. Scale bars: 50 μm (A, C and E), 100 μm (B and D).

3.4. Histological analysis

Cross-sectional slices stained with haematoxylin and eosin are shown in Fig. 4. As shown in Fig. 4(A) and (B) respectively, one CM cell sheet has a thickness of approximately 40–50 μm and a decellularised SIS is approximately 300–500 μm thick. No remnant cells were detected in the decellularised SIS. Seeded Percoll CM attached to the decellularised SIS (Fig. 4(C)). Layered CM cell sheets adhered to each other or to the CM-seeded SIS (Fig. 4(D) and (E)), and a seeded SIS layered with three CM sheets measured approximately 600–800 μm thick.

Immunohistochemical analysis with phalloidin and anti-α-sarcomeric actinin confirmed that the seeded Percoll CM aligned parallel to the longitudinal axis of the SIS (Fig. 5(A) and (B)). Although CM in the detached cell sheet appeared disordered and without alignment (Fig. 5(C)), once attached to the seeded SIS, the CM within the cell sheet aligned in a similar direction to the Percoll CM (along the longitudinal axis of the SIS) (Fig. 5(D) and (E)). These findings support the macroscopic and microscopic observations reported above.

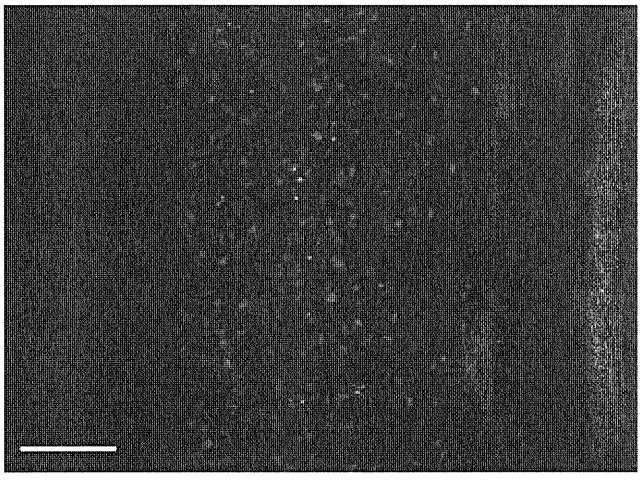

Fig. 6. Anti-connexin 43 staining revealed gap-junctions throughout three-layered cardiomyocyte sheets on seeded small-intestinal submucosa (SIS). Nuclei were counterstained with DAPI. Scale bars: 100 μm.

Anti-α-sarcomeric actinin staining also revealed the typical striated pattern of the CM in both the Percoll-seeded cells on SIS and in the CMs of the attached sheets (Fig. 5(B), (D) and (E)). Immunohistochemical staining with anti-connexin 43 demonstrated a diffuse expression of connexin 43 within the three-layered CM sheets on the seeded SIS (Fig. 6).

4. Discussion

Cell-transplantation therapy, to treat damaged myocardium, has been widely studied and has resulted in positive, albeit limited, effects in clinical trials [16]. Despite early success, problems still remain including method of cell delivery, poor graft survival, functional integration and post-transplantation arrhythmias [17]. Moreover, changes in the ECM, which are regarded to play a pivotal role for cell survival, differentiation, proliferation, metabolism and integrative function, are not taken into consideration with this intervention [18]. The emergence of a second regenerative therapy using a combination of cells and ECM provide greater advantages towards the engineering of a three-dimensional functional myocardial patch [18,19]. To this point, the present study demonstrated the feasibility of generating a contractile myocardial patch by combining a decellularised biological matrix (SIS) with CM cell sheets. Moreover, we show that CM sheets can be layered on SIS without disrupting contractile alignment and function of the CM. Thus, our results represent an important intermediate step towards the engineering of a complex, multilayered contractile myocardial patch.

Decellularised SIS is an ideal matrix for tissue engineering and remodelling due in part, to its intact ECM. The ECM of SIS consists primarily of collagens (types I, III and VI), and also glycosaminoglycans, for example, hyaluronic acid, chondroitin sulphate A and B, heparin, and heparan sulphate, and glycoproteins, for example, fibronectin. In addition, several cytokines are produced, including basic fibroblast growth factor and transforming growth factor-β, which together induce cellular migration, proliferation and differentiation, early capillary ingrowth and ultimately, endothelialisation. In addition, decellularised SIS has been previously characterised as a complete absorbable biocompatible framework with a high resistance towards infection [20,21]. Moreover, inherent SIS fibre alignment is along the longitudinal axis of the small intestine [22,23], which enables us to induce a 'preferred' cellular alignment without mechanical stimulation. Typically, the native cell alignment in an artificial tissue-engineered system is accomplished either by mechanical stimulation or by using a patterned scaffold requiring complex devices or materials [1,4]. When SIS is used; however, it leads to an orthotropic mechanical behaviour of the scaffold, with the preferred fibre direction showing great stiffness and strength [22,23].

Cell sheet engineering is a well-established technique using cells from various sources, and has already been investigated in a clinical setting [24]. CM cell sheets are unique due to their contractile ability. The most distinct advantage of CM cell sheet engineering is that they can be easily layered while maintaining electrically communicative pulsation supported through gap-junctions [7,8]. To this point, anti-connexin 43 immunohistochemistry revealed diffuse gap-junctions within the three-layered CM sheets on the CM-seeded SIS. This abundant detection of connexin 43 suggested the formation of an electrical syncytium throughout the cell sheets and connection with CM seeded on SIS. This finding, in addition to the intact ECM of the SIS, provides strong support for the coupling of these two technologies.

Despite initial success, additional questions with respect to the detailed character of a tissue-engineered heart patch remain unanswered. First, the strength and durability of the contractile forces generated by the layered CM sheets are unknown. These assessments are crucial as the patch is being generated to replace scar tissue in the left ventricle of the heart. A previous study has shown that SIS itself or a similar ECM, for example, porcine urinary bladder matrix, could substitute for the right ventricular wall [11] or even the left ventricular wall [12] in a large animal model. However, in that study, the patches were implanted as four ECM-layered patches based on the idea that the mechanical behaviour of a single layer of SIS is insufficient for most load-bearing applications [22]. Recently, our colleagues reported a successful implantation of an autologous vascularised matrix from a porcine small bowel segment without mucosa to the right ventricular wall of the pig [25]. While it differs from our myocardial construct in its characteristics, its thickness is comparable. The results from this study suggest that one SIS layer may, in fact, be sufficient.

A second question is whether the ECM provided by the SIS is similar or adaptable to a native-like ECM, to support the contractility of the ventricle [25]. While the CM cell sheet has an ECM of ventricular origin, the effect of the intestinal ECM on myocardial function has not been determined. Cell source is the subject of the third question. For clinical application, the use of autologous, allogenic or xenogenic CMs may be problematic. Of course, this matter is universal in cardiac tissue engineering and most cell-based therapies. To this point, embryonic and adult stem cells, or induced pluripotent stem cell-based approaches will play a central role in the near future [1].

Finally, the engineering of myocardial heart patch with CM cell sheets is limited by the thickness generated through sheet stacking. In this study, a myocardial patch with a thickness of roughly 800 μm was built. Although possible, more cell sheets can be continuously layered; however, supplying sufficient oxygen and nutrients will challenge the viability of a thicker construct. Although these issues will be addressed to determine the future clinical application, the present preliminary study shows the novel development of a pulsatile, thicker myocardial patch with unidirectional contractions and proposes a new strategy for regenerative therapy for cardiac dysfunction.

In conclusion, by combining a CM-seeded matrix with CM sheets, a multilayered and contracting myocardial graft was successfully generated. Moreover, our novel myocardial patch is a good foundation for our ultimate goal; a vascularised three-dimensional myocardial graft.

References

[1] Eschenhagen T, Zimmermann WH. Engineering myocardial tissue. Circ Res 2005;97:1220–31.

[2] Haverich A. Cardiac tissue engineering. Eur J Cardiothorac Surg 2008;34:227–8.
[3] Zimmermann WH, Didie M, Döker S, Melnzchenko I, Naito H, Rogge C, Tiburcz M, Eschenhagen T. Heart muscle engineering: an update on cardiac muscle replacement therapy. Cardiovasc Res 2006;71:419–29.
[4] Zhao YS, Wang CY, Li DX, Zhang XZ, Qiao Y, Guo XM, Wang XL, Dun CM, Dong LZ, Song Y. Construction of a unidirectionally beating 3-dimensional cardiac muscle construct. J Heart Lung Transplant 2005;24:1091–7.
[5] Kofidis T, Akhyari P, Boublik J, Theodorou P, Martin U, Ruhparwar A, Fischer S, Eschenhagen T, Kubis HP, Kraft T, Leyh R, Haverich A. In vitro engineering of heart muscle: artificial myocardial tissue. J Thorac Cardiovasc Surg 2002;124:63–9.
[6] Bär A, Haverich A, Hilfiker A. Cardiac tissue engineering: "reconstructing the motor of life". Scand J Surg 2007;96:154–8.
[7] Shimizu T, Yamato M, Isoi Y, Akutsu T, Setomaru T, Abe K, Kikuchi A, Umezu M, Okano T. Fabrication of pulsatile cardiac tissue grafts using a novel 3-dimensional cell sheet manipulation technique and temperature-responsive cell culture surfaces. Circ Res 2002;90:e40.
[8] Miyagawa S, Sawa Y, Sakakida S, Taketani S, Kondoh H, Memon IA, Imanishi Y, Shimizu T, Okano T, Matsuda H. Tissue cardiomyoplasty using bioengineered contractile cardiomyocyte sheets to repair damaged myocardium: their integration with recipient myocardium. Transplantation 2005;80:1586–95.
[9] Hata H, Matsumiya G, Miyagawa S, Kondoh H, Kawaguchi N, Matsuura N, Shimizu T, Okano T, Matsuda H, Sawa Y. Grafted skeletal myoblast sheets attenuate myocardial remodeling in pacing-induced canine heart failure model. J Thorac Cardiovasc Surg 2006;32:918–24.
[10] Hodde J. Naturally occurring scaffolds for soft tissue repair and regeneration. Tissue Eng 2002;8:295–308.
[11] Badylak S, Obermiller J, Geddes L, Matheny R. Extracellular matrix for myocardial repair. Heart Surg Forum 2003;6:E20–26.
[12] Robinson KA, Li J, Mathison M, Redkar A, Cui J, Chronos NA, Matheny RG, Badylak SF. Extracellular matrix scaffold for cardiac repair. Circulation 2005;112:I135–143.
[13] Meezan E, Hjelle JT, Brendel K. A simple versatile; nondisruptive method for the isolation of morphologically and chemically pure basement membranes from several tissues. Life Sci 1975;17:1721–32.
[14] Wollert KC, Taga T, Saito M, Narazaki M, Kishimoto T, Glembotski CC, Vernallis AB, Heath JK, Pennica D, Wood WI, Chien KR. Cardiotrophin-1 activates a distinct form of cardiac muscle cell hypertrophy. Assembly of sarcomeric units in series VIA gp130/leukemia inhibitory factor receptor-dependent pathways. J Biol Chem 1996;271:9535–45.
[15] Iwaki K, Sukhatme VP, Shubeita HE, Chien KR. Alpha- and beta-adrenergic stimulation induces distinct patterns of immediate early gene expression in neonatal rat myocardial cells. fos/jun expression is associated with sarcomere assembly; Egr-1 induction is primarily an alpha 1-mediated response. J Biol Chem 1990;265:13809–17.
[16] Hagège AA, Marolleau JP, Vilquin JT, Alhéritière A, Peyrard S, Duboc D, Abergel E, Messas E, Mousseaux E, Schwartz K, Desnos M, Menasché P. Skeletal myoblast transplantation in ischemic heart failure: long-term follow-up of the first phase I cohort of patients. Circulation 2006;114(1 Suppl.):I108–13.
[17] Menasché P, Alfieri O, Janssens S, McKenna W, Reichenspurner H, Trinquart L, Vilquin JT, Marolleau JP, Seymour B, Larghero J, Lake S, Chatellier G, Solomon S, Desnos M, Hagège AA. Circulation 2008;117:1189–200.
[18] Akhyari P, Kamiya H, Haverich A, Karck M, Lichtenberg A. Myocardial tissue engineering: the extracellular matrix. Eur J Cardiothorac Surg 2008;34:229–41.
[19] Chachques JC, Trainini JC, Lago N, Cortes-Morichetti M, Schussler O, Carpentier A. Myocardial Assistance by Grafting a New Bioartificial Upgraded Myocardium (MAGNUM trial): clinical feasibility study. Ann Thorac Surg 2008;85:901–8.
[20] Lindberg K, Badylak SF. Porcine small intestinal submucosa (SIS): a bioscaffold supporting in vitro primary human epidermal cell differentiation and synthesis of basement membrane proteins. Burns 2001;27:254–66.
[21] Mertsching H, Walles T, Hofmann M, Schanz J, Knapp WH. Engineering of a vascularized scaffold for artificial tissue and organ generation. Biomaterials 2005;26:6610–7.
[22] Badylak SF. The extracellular matrix as a biologic scaffold material. Biomaterials 2007;28:3587–93.
[23] Sacks MS, Gloeckner DC. Quantification of the fiber architecture and biaxial mechanical behavior of porcine intestinal submucosa. J Biomed Mater Res 1999;46:1–10.
[24] Yang J, Yamato M, Shimizu T, Sekine H, Ohashi K, Kanzaki M, Ohki T, Nishida K, Okano T. Reconstruction of functional tissues with cell sheet engineering. Biomaterials 2007;28:5033–43.
[25] Tudorache I, Kostin S, Meyer T, Teebken O, Bara C, Hilfiker A, Haverich A, Cebotari S. Viable vascularized autologous patch for transmural myocardial reconstruction. Eur J Cardiothorac Surg 2009;36:306–11.

Appendix A. Conference discussion

Dr P. Menasche (*Paris, France*): Thank you and your colleagues for providing additional evidence that the expected benefits of cell therapy are likely to be enhanced by some form of cell scaffolding. That said, I have two questions.

The first is that if one looks at the improvement in the contraction patterns in your composite biomaterial, the composite – I mean the SIS plus the cell sheets, it turns out that it might simply reflect the fact that you had many more cells in your combined biomaterial compared with either treatment alone. You had five times more cells in the combined scaffold. So keeping in mind that the widespread clinical application of any technique requires it to be as simple as possible, my naive question is: Would it be conceivable that you would get a similar result if you simply increased the cell-seeding density on your SIS to match the final number of cells that you have got when you have combined the two materials? And that would probably be true also for explaining the increased thickness. Again you had such a disparity in the numbers of cells between the groups that it might be one explanation for your results. So is there any rationale for combining the two scaffolds? And you probably should tell us what is the contribution of a given material to the other instead of using just a single material with more cells, contractile cells, on board.

My second question is that you have shown us that there was some expression of connexin 43. Did you do some dye experiments documenting that you have an effective transmission of the impulses from one cell to the other? And more importantly, we realize that this is an in vitro study, but do you have any in vivo data allowing you to speculate on how these epicardially-delivered cells would couple with the underlying host cardiomyocytes, because obviously this is critical.

Dr Hata: As to your first question, we seeded about 180,000 cells/sq cm onto SIS and 400,000 cells/cm sq/cardiomyocyte sheet. So, as you mentioned, these cell numbers do not match. I think we need more cells to generate cell sheet than to seed on SIS. We seeded cardiomyocyte on SIS for the sake of the affinity for cardiomyocyte sheets, and we tested also cardiomyocyte sheet on un-seeded SIS but that construct did not contract longer than 4 days in a defined direction.

And the reason we used SIS as a scaffold is not only to gain thickness, but also looking toward the next step in our research utilizing vascularised SIS, so-called BioVaM. We would like to use such vascularised SIS as our next step, so we tested the feasibility of SIS in combination with cell sheets.

And as for the second question, in fact we didn't do any functional testing or *in vivo* studies. I think it may be the focus of our future studies. However, when we think about the animal model, we used here neonatal rat cardiomyocytes. So when we use a large animal model, we must think about a suitable cell source, such as iPS cells.

And you mentioned connexin 43 – I'm sorry what was your question?

Dr Menasche: The question is: Do you have any data, or can you speculate, on how cells which are delivered on the epicardium, which would be delivered on the epicardium, how you think they could couple with the cardiomyocytes of the recipient heart which are underneath?

Dr Vaage (*Oslo, Norway*): Does Axel Haverich want to comment on this?

Dr Haverich: We did implant, also in large animal preparations, the SIS only, and we have seen coupling there. We only did these experiments to increase the thickness. Because we can do right atrial, right ventricular replacement at this point, but for left ventricular replacement we need to increase the thickness and this is why we have this combined approach. We have done electrophysiology and put a pacemaker lead on one side of the graft *in vitro* and have seen propagation of the impulse. With regard to your connexin question, we have seen propagation of the contraction towards the other end of the graft. So there is electrophysiological contact between the cells.

Appendix B. Supplementary data

Supplementary data associated with this article can be found, in the online version, at doi:10.1016/j.ejcts.2010.02.009.

Circulation Journal
Official Journal of the Japanese Circulation Society
http://www.j-circ.or.jp

ORIGINAL ARTICLE
Cardiovascular Surgery

Risk Factor Analysis of Long-Term Support With Left Ventricular Assist System

Shunsuke Saito, MD; Goro Matsumiya, MD; Taichi Sakaguchi, MD; Shigeru Miyagawa, MD; Yasushi Yoshikawa, MD; Takashi Yamauchi, MD; Toru Kuratani, MD; Yoshiki Sawa, MD

Background: This study was designed to elucidate the key factors for successful long-term support with a left ventricular assist system (LVAS) in the situation where heart transplantation is rarely available.

Methods and Results: From 1992 to 2008, 106 patients underwent 121 LVAS implantations at Osaka University Hospital (Toyobo: 77; Novacor: 18; HeartMate: 14; Jarvik2000: 8; EvaHeart: 2; DuraHeart: 2). Risk factors for infection were early on the former implanted period (odds ratio (OR) 3.30), Toyobo (OR 2.25), mechanical right heart support (OR 2.30) and cardiopulmonary bypass time (OR 1.01). Left atrium as the inflow site was the risk factor for cerebrovascular events (OR 2.84). Older age (OR 1.04) and mechanical right heart support (OR 4.70) were risk factors for mortality. Risk factors for requiring mechanical right heart support were preoperative extracorporeal membranous oxygenation support (OR 5.641), serum total bilirubin (OR 1.11) and serum creatinine (OR 2.46). On the basis of the risk analysis for mortality, patients were divided into 2 subgroups (low and high risk) and the respective cumulative survival at 1 year after LVAS implantation was 75.2% and 25.0%.

Conclusions: Appropriate selection of device, patient and the timing of implantation and less invasive operation are important for successful long-term LVAS support. (*Circ J* 2010; **74:** 715–722)

Key Words: Bridge to transplantation; Destination therapy; Left ventricular assist system; Long-term support; Risk analysis

The left ventricular assist system (LVAS) has been successfully used as treatment of end-stage heart failure, mainly as a bridge to transplantation.[1] From successful experiences with using LVAS in heart transplantation candidates, permanent use of LVAS has recently also become realistic in the United States and Europe.[2,3] Several sophisticated devices have been developed over the years and are suitable for different patients with different therapeutic objectives. After many years of experiences with these life-saving devices, researchers have suggested that appropriate patient selection and device selection are essential for effective use of LVAS.[4–7] In Japan, however, the special situation of heart transplantation and very limited device availability have made the indication and timing of LVAS implantation somewhat different from other countries.[8] Because of the extremely severe shortage of donor hearts, heart failure patients in Japan have to wait for heart transplantation for approximately 2 years on average with LVAS support.[8,9] To make the situation worse, the only commercially available device in this country has been the Toyobo LVAS, which is a paracorporeal pneumatic-type LVAS that was initially designed for short-term support.[10,11] The available support flow is smaller than with other types of implantable devices, and the patient cannot leave the hospital because the driving unit is designed for the inpatient setting. Most of the heart transplantation candidates have to wait for donor hearts for a long time on this device, dealing with repeat complications such as infection and thromboembolism.

Editorial p624

Despite this special situation, risk analysis of LVAS treatment in this country has been rarely conducted, so the purpose of this study was to elucidate the predictors of major adverse events and mortality with LVAS treatment in Japan.

Methods

From April 1992 to November 2008, 106 patients underwent a total of 121 LVAS implantations at Osaka University Hospital. The indication for LVAS implantation was irreversible end-stage heart failure with New York Heart Association (NYHA) class IV symptoms and imminent or already present end-organ dysfunction despite optimal medical therapy including inotropic agents. The patients' demographics are summarized in **Table 1**. The number of LVAS implantations

Received October 5, 2009; revised manuscript received December 16, 2009; accepted December 17, 2009; released online February 17, 2010 Time for primary review: 30 days

Division of Cardiovascular Surgery, Department of Surgery, Osaka University Graduate School of Medicine, Suita, Japan
Mailing address: Yoshiki Sawa, MD, Division of Cardiovascular Surgery, Department of Surgery, Osaka University Graduate School of Medicine (E1), 2-2 Yamada-oka, Suita 565-0871, Japan. E-mail: sawa@surg1.med.osaka-u.ac.jp

ISSN-1346-9843 doi:10.1253/circj.CJ-09-0747

Table 1. Clinical Characteristics of the Patients Requiring LVAS	
Male (%)	85/106 (80.2)
Mean age (years)	40.2±15.6 (range 7–73)
Mean body surface area (m^2)	1.60±0.23 (range 0.80–2.32)
Etiology of heart failure, n (%)	
Idiopathic cardiomyopathy	69 (65.1)
Ischemic cardiomyopathy	23 (21.7)
Myocarditis	8 (7.5)
Secondary cardiomyopathy	5 (4.7)
Others	1 (0.9)
Preoperative status n (%)	
Mechanical ventilation	69 (65.1)
Intra-aortic balloon pump	63 (59.4)
ECMO	39 (36.8)
Renal dysfunction	
Serum creatinine >2.0 mg/dl	27 (25.5)
Hemodialysis	11 (10.4)
Liver dysfunction	
Serum total bilirubin >3.0 mg/dl	45 (42.5)
Blood chemistry	
BUN (mg/dl)	36.5±24.3
Creatinine (mg/dl)	1.6±1.1
AST (IU/L)	263±821
ALT (IU/L)	245±717
Total bilirubin (mg/dl)	4.9±6.8
Total protein (mg/dl)	6.3±0.9
Albumin (mg/dl)	3.3±0.6
White blood cell ($\times 10^3/\mu l$)	10.4±5.7
CRP (mg/dl)	8.5±9.1
Brain natriuretic peptide (pg/ml)	1,416±1,116
Echocardiography data	
LVDd (mm)	66.9±12.3
Ejection fraction (%)	19.7±11.1
Mitral regurgitation ≥III	37 (38.9%)
Right heart catheterization	
Heart rate (beats/min)	104±24
Systolic blood pressure (mmHg)	93±18
Central venous pressure (mmHg)	11.2±6.0
Systolic pulmonary artery pressure (mmHg)	48±16
Pulmonary capillary wedge pressure (mmHg)	25±10
Cardiac index ($L \cdot min^{-1} \cdot m^{-2}$)	1.9±0.6

LVAS, left ventricular assist system; ECMO, extracorporeal membranous oxygenation; AST, aspartate aminotransferase; ALT, alanine aminotransferase; CRP, C-reactive protein; LVDd, left ventricular diastolic dimension.

has increased since 1999 (**Figure 1**), when the first heart transplantation from a brain-dead donor was performed in Japan. The most commonly used device was the Toyobo paracorporeal pneumatic LVAS.[10,11] Since the left ventricular apical drainage system became available in 1999, we began using that as the primary choice. Since 1994, implantable LVAS, such as the HeartMate (Thoratec Corp, Pleasanton, CA, USA) and Novacor (WorldHeart Corp, Oakland, CA, USA), also became available to us, but these devices were used in a limited number of patients, mainly patients who had been registered as heart transplantation candidates with sufficient body size (body surface area >1.50 m^2). More recently, non-pulsatile LVAS such as the Jarvik 2000 (Jarvik Heart, Inc, New York, NY, USA), EvaHeart (SunMedical Technology Research, Nagano, Japan) and DuraHeart (Terumo Heart, Inc, Ann Arbor, MI, USA) were also used as part of a clinical trial, but the indication of the new devices was limited to patients without significant complications. As a result, the Toyobo LVAS was selected for patients with a smaller body size or for those with significant preexisting complications who could not be registered as transplantation candidates or with acute deterioration of heart failure.

Implantation procedures were performed either through a median sternotomy or left thoracotomy as previously described.[12–14] We prefer performing all procedures without cardioplegic cardiac arrest unless the left ventricle is seriously damaged by acute myocardial infarction or a left ventricular thrombus is identified. To facilitate future LVAS explantation, we aggressively perform concomitant procedures such as left ventricular restoration, mitral valve repair, and cardiac

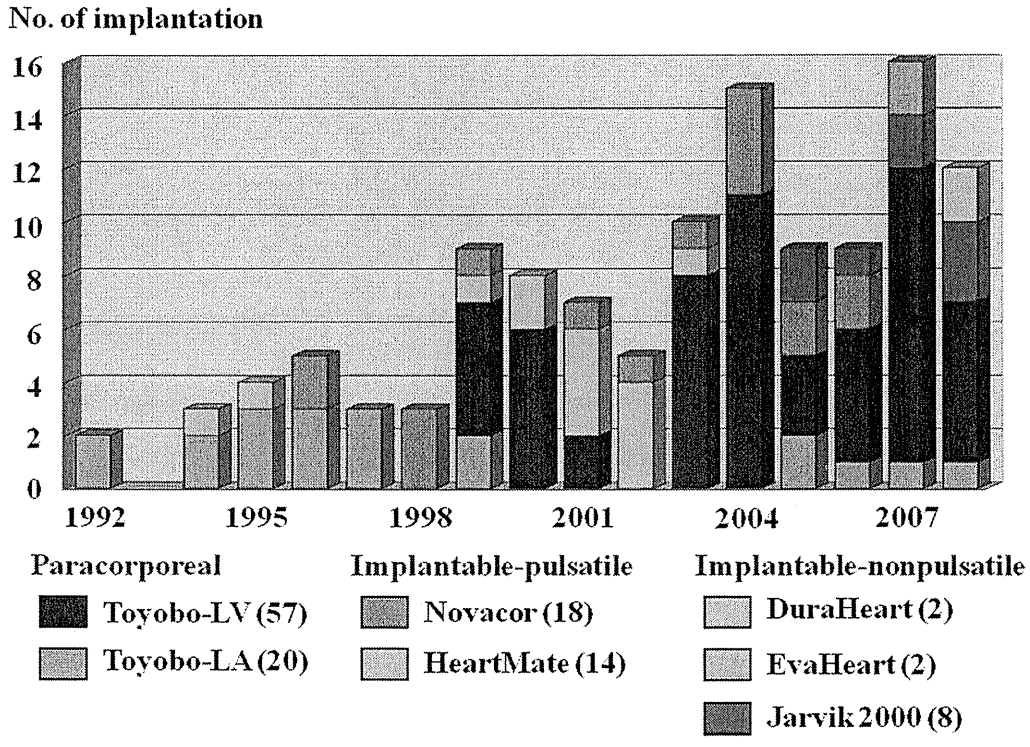

Figure 1. LVAS implantation at Osaka University Hospital. Toyobo-LV, Toyobo LVAS with left ventricular apical drainage; Toyobo-LA, Toyobo LVAS with left atrial drainage; LVAS, left ventricular assist system.

Table 2. Clinical Outcomes of the Patients Requiring LVAS

	n (%)
Transplanted	17 (16.0%)
Abroad	4
At Osaka University Hospital	13
Novacor	6
Toyobo	5
HeartMate	3
Jarvik 2000	3
Removal of LVAS	18 (17.0%)
Emergency removal	6
Died after removal	3
Died after re-LVAS	3
Scheduled removal	12
re-LVAS	3
Ongoing	17
Hospitalized	11
At home	6
Cause of death	
Sepsis	17
Multiple organ failure	16
Cerebral bleeding	13
Cerebral infarction	12
Other	5

Abbreviation see in Table 1.

Table 3. Device-Related Complications in the Patients Requiring LVAS

	n (%)
Infection	
Positive blood culture	46 (43.4%)
Driveline exit site infection	36 (34.0%)
Mediastinitis/pump pocket infection	15 (15.1%)
Cerebrovascular events	
Cerebral bleeding	29 (27.4%)
Cerebral infarction	28 (26.4%)
Reoperation for bleeding/cardiac tamponade	28 (26.4%)
Respiratory failure (tracheostomy)	30 (28.3%)
Renal failure (temporary hemodialysis)	30 (28.3%)

Abbreviation see in Table 1.

resynchronization therapy, if indicated. Concomitant procedures during LVAS implantation included mitral valve annuloplasty in 29 patients, tricuspid annuloplasty in 29, biventricular lead implantation in 10, left ventricular restoration in 5, aortic valve replacement in 3, and coronary artery bypass grafting in 2. If LVAS filling was poor when weaning from cardiopulmonary bypass with adequate right atrial pressure and support for right ventricle using nitric oxide inhalation and catecholamine, right ventricular assist using an extracorporeal membranous oxygenation (ECMO-RVAS) was established with right atrial appendage and pulmonary artery cannulation. If right heart failure was so severe that the surgeon considered weaning from the ECMO-RVAS impossible within 1 week, a RVAS using a Toyobo pump was

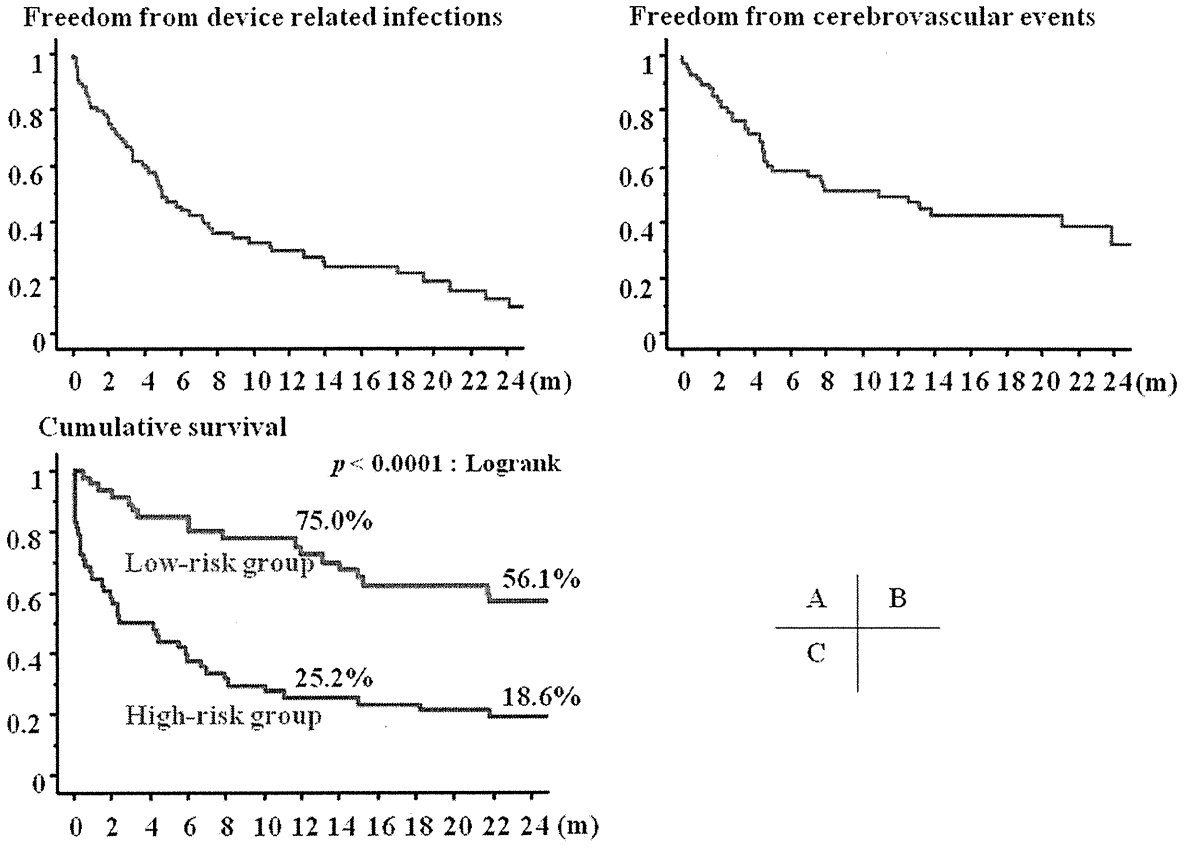

Figure 2. (**A**) Freedom from device-related infections (positive blood culture, driveline infection, mediastinitis and pump pocket infection). (**B**) Freedom from cerebrovascular events (cerebral bleeding and cerebral infarction). (**C**) Cumulative survival of high-risk group and low-risk group (see text for definitions).

established instead of ECMO.

In the first 24 h postoperatively the patients received no anticoagulation therapy. Thereafter, if there was no significant drainage from the chest tube, continuous heparin infusion was started and the activated partial thromboplastin time was maintained at 1.5- to 2-fold the normal value. Long-term anticoagulation consisted of coumadin (dosage according to international normalized ratio 2.5–3.5), and aspirin 100–200 mg/day. Since 2002 ticlopidine 200 mg/day has been added as antiplatelet therapy. Patients with the HeartMate LVAS received only aspirin.

The hospital records of the 106 patients were retrospectively reviewed. Preoperative status, operative strategies, and clinical outcomes were evaluated. This study was approved by the ethics committees of the Osaka University Graduate School of Medicine. All patients gave written informed consent.

Statistical Analysis

Kaplan-Meier analysis was used to estimate the event-free provability over time. The comparison of the survival rate of the 2 groups was done by log-rank (Mantel-Cox) analysis with P values less than 0.05 considered to be significant. From the patients' preoperative parameters and operative procedures, predictors of device-related infection, cerebrovascular events after LVAS implantation and mortality were evaluated using a Cox hazard model. Predictors of requiring mechanical right heart support during operation in order to wean off the cardiopulmonary bypass were evaluated using a logistic regression model.

Results

A total of 29 patients required mechanical right heart support during the operation. ECMO-RVAS was implanted in 22 of them and the Toyobo RVAS in the others. Of the 22 patients who underwent ECMO-RVAS support, right heart function recovered and RVAS was removed in 10 patients, ECMO-RVAS was switched to the Toyobo RVAS in 4 and the other 8 died with ECMO-RVAS support. Two patients underwent Toyobo RVAS implantation after LVAS implantation because of persistent right heart failure. None of the patients with the Toyobo RVAS survived to transplantation or recovery. The median duration of biventricular support with Toyobo pumps was 129 days (range 19–353 days).

Clinical outcomes are summarized in **Table 2**. Only 17 patients were successfully bridged to heart transplantation. The median duration of LVAS support of those who were bridged to transplantation was 591 days (range 21–1,233 days). LVAS was removed in 18 patients: 6 underwent emergency LVAS removal because of serious complications such as cerebral bleeding or infections and 3 of them died after LVAS removal; the other 3 died after LVAS reimplantation.

Table 4. Risk Factors for Device-Related Infection (Cox Hazard Model)

	Univariate	Multivariate	OR (95%CI)
	P value	P value	
Implanted period (~2002)	0.0008	0.0004	3.299 (1.694–6.425)
White blood cells	0.0061	NS	–
Device (Toyobo)	0.0008	0.0469	2.251 (1.011–5.009)
Inflow site (left atrium)	0.0145	NS	–
Right heart support*	0.0004	0.0291	2.297 (1.089–4.847)
Cardiopulmonary bypass time	0.0009	0.0064	1.009 (1.002–1.013)

Entry probability set at 0.10.
*Requiring right heart support to wean off cardiopulmonary bypass during the operation.
OR, odds ratio; CI, confidence interval.

Table 5. Risk Factors for Cerebrovascular Events (Cox Hazard Model)

	Univariate	Multivariate	OR (95%CI)
	P value	P value	
White blood cells	0.0505	NS	–
Preoperative ECMO support	0.0369	NS	
Concomitant mitral valve surgery	0.0783	NS	–
Device (Toyobo)	0.0125	NS	–
Inflow site (left atrium)	0.0039	0.0263	2.838 (1.131–7.123)

Entry probability set at 0.10.
Abbreviations see in Tables 1,4.

Table 6. Risk Factors for Mortality (Cox Hazard Model)

	Univariate	Multivariate	OR (95%CI)
	P value	P value	
Implanted period (~2002)	0.0261	NS	–
Age at implantation	0.0142	0.0083	1.039 (1.010–1.069)
Etiology (idiopathic)	0.0613	NS	–
White blood cells	0.0507	NS	–
Total bilirubin	0.0192	NS	–
Creatinine	0.0376	NS	–
Albumin	0.0057	NS	–
Preoperative ECMO support	0.0079	NS	–
Preoperative hemodialysis	<0.0001	NS	–
Device (Toyobo)	0.0003	NS	–
Inflow site (left atrium)	0.0011	NS	–
Right heart support*	<0.0001	0.0034	4.698 (1.668–13.230)
Cardiopulmonary bypass time	<0.0001	NS	–

Entry probability set at 0.10.
*Requiring right heart support to wean off cardiopulmonary bypass during the operation.
Abbreviations see in Tables 1,4.

LVAS was removed in 12 patients because their own heart function recovered and all of them are alive. There was recurrence of heart failure in 3 patients, requiring reimplantation of LVAS. Two of them underwent heart transplantation and the other is ongoing.

Device-related complications are summarized in **Table 3**. Nearly half of the patients (43.4%) had a positive blood culture at least once. Driveline exit site infection was observed in 34.0% of patients and mediastinitis or pump pocket infection in 15.1%. **Figure 2A** shows freedom from device-related infections. Although the infectious events occurred most frequently in the first 6 months after LVAS implantation, they continued to occur thereafter. Predictors of device-related infections were evaluated using a Cox hazard model (**Table 4**). Multivariate analysis revealed that early implanted period, Toyobo, requiring mechanical right heart support to wean off cardiopulmonary bypass, and longer cardiopulmonary bypass time were the independent risk factors for device-related infections.

Cerebral bleeding and cerebral infarction were observed in 27.4% and 26.4% of patients, respectively, including overlap (**Table 3**). **Figure 2B** shows freedom from cerebrovascular events. As with infection, cerebrovascular events occurred most frequently in the first 6 months after LVAS implantation, but continued to occur thereafter, although the frequency seemed to decrease after 1 year. Multivariate analysis using Cox hazard model revealed that the inflow site (ie, left atrium) was the independent risk factor (**Table 5**).

Table 7. Risk Factors for Right Heart Failure (Logistic Regression Model)

	Univariate	Multivariate	OR (95%CI)
	P value	P value	
Female	0.0432	NS	–
Etiology (idiopathic)	0.0064	NS	–
Total bilirubin	0.0058	0.0337	1.113 (1.008–1.229)
Creatinine	0.0039	0.0052	2.460 (1.308–4.630)
C-reactive protein	0.0048	NS	–
Preoperative intubation	0.0009	NS	–
Preoperative ECMO support	<0.0001	0.0101	5.641 (1.509–21.086)
Device (Toyobo)	0.0022	NS	–

Entry probability set at 0.10.
Abbreviations see in Tables 1,4.

The most common causes of death were multiple organ failure and sepsis, which were already present preoperatively in the majority of cases (**Table 2**). Cerebral infarction and bleeding were the other leading causes of death. Predictors of mortality were evaluated using a Cox hazard model (**Table 6**). By multivariate analysis, older age at implantation and mechanical right heart support requirement were the independent risk factors for death. As the requirement of mechanical right heart support was revealed to be the strongest risk factor for death (odds ratio (OR) 4.698) and also the independent risk factor for device-related infections, predictors for requiring mechanical right heart support to wean off the cardiopulmonary bypass during LVAS implantation were evaluated using a logistic regression model (**Table 7**). Multivariate analysis revealed preoperative serum total bilirubin and creatinine levels, and preoperative ECMO support were the independent risk factors.

On the basis of the risk analysis for death, patients were divided into 2 subgroups: high and low risk. The high-risk group included patients with at least 1 of age at implantation (≥60 years) and/or mechanical right heart support. The low-risk group included patients with neither of these risk factors. There was a remarkable difference between the groups in the survival rate after LVAS implantation (**Figure 2C**). Cumulative survival in the low-risk group was 75.0% at 1 year after LVAS implantation and 56.1% at 2 years.

Discussion

In a study of the Novacor European Registry, Deng et al reported that respiratory failure with septicemia, preexisting right heart failure, age at implantation, acute postcardiotomy and acute infarction were predictors of mortality after LVAS implantation by multivariate analysis.[4] Cumulative survival was significantly higher in the group of patients without any of these risk factors (low-risk group) than in the group of patients with at least 1 risk factor (high-risk group). Two of the risk factors (right heart failure and age at implantation) are the same as those detected as predictors of mortality in our study. The influence of these factors on the patient survival after LVAS implantation was also similar: cumulative survival of the low-risk group and high risk group at 1 year was 60.3% and 24.1%, respectively, in Deng's report, and 75.0% and 25.2%, respectively, in our study. The different points of the 2 studies are the number of patients that underwent heart transplantation and the duration of LVAS support until heart transplantation. In Deng's report, 155 of 366 patients (42.3%) underwent heart transplantation and the median time on LVAS until heart transplantation was 139 days in the low-risk group and 88 days in the high-risk group, whereas in our study only 17 of 106 patients (16.0%) underwent heart transplantation and the median time on LVAS until heart transplantation was 591 days.

In addition to the severe shortage of donor hearts, limited device selection is a significant disadvantage of LVAS treatment in Japan. Although it is important to select devices according to the predicted duration of support,[6] the Toyobo LVAS is the only commercially available LVAS today and we have no choice but to use this paracorporeal pneumatic device in most patients, no matter how long the duration of the support is expected to be. In this study, the Toyobo LVAS was detected as an independent risk factor for device-related infection. Implantable LVAS is considered to reduce the risk of device-related infection compared with paracorporeal LVAS,[15] and it was reported more recently that device-related infection is reduced significantly by smaller continuous flow devices.[16] Patients with the Toyobo LVAS cannot leave hospital because this device is designed for the inpatient setting. In addition to the frequent infectious events with the paracorporeal device in the acute phase, nosocomial infection may have played a significant role in infections in the late phase (infectious events after 6 months: **Figure 2A**). The incidence of infections in the late phase might be reduced if patients could go home with an implantable LVAS. The other predictors of device-related infection in previous reports include renal dysfunction,[17] hypo-albuminemia,[18] and diabetes mellitus.[19]

The other important complication of LVAS treatment is cerebrovascular events, and it is known that the risk increases with a longer LVAS support period.[20] This complication seems to be device- and anti-coagulation therapy-related, and none of the patients' preoperative factors was detected as a predictor of post-LVAS cerebrovascular events in this study. The only predictor of cerebrovascular events was left atrial drainage. When left heart bypass is established between the left atrium and ascending aorta in a heart with poor contraction, stagnation of the blood stream and thrombus formation tends to occur in the left ventricle, resulting in cerebral thromboembolism. In this study, the left atrium was selected as the inflow site in patients before the left ventricular apical drainage system was introduced in 1999, and thereafter we used the left ventricular apex as the inflow site, unless there was a special reason not to, such as not being suitable because of previous left ventricular plasty or fragility resulting from acute myocardial infarction.

Right heart failure is also known to be a significant risk

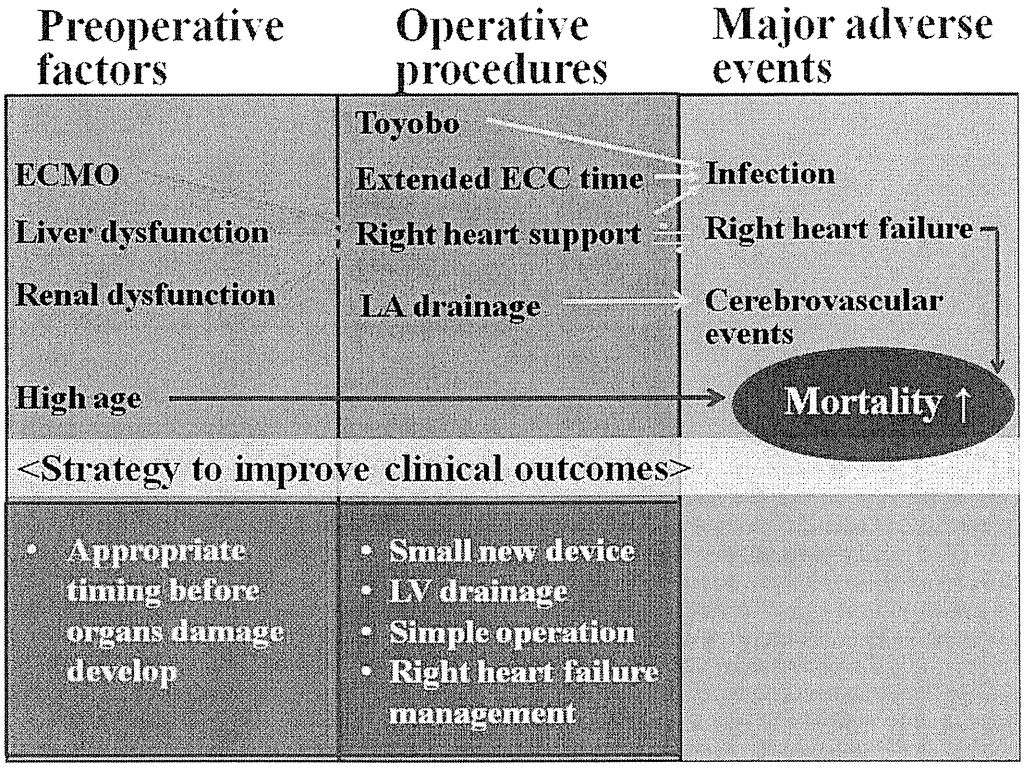

Figure 3. Summary of the study findings showing the preoperative and operative independent risk factors for major adverse events and mortality. The strategies for improving LVAS treatment are derived from these findings. ECMO, extracorporeal membranous oxygenation; LA, left atrium; LV, left ventricle; LVAS, left ventricular assist system.

factor for unsuccessful LVAS treatment,[21–24] and several studies have revealed the preoperative risk factors for developing right heart failure after LVAS implantation.[21–25] Researchers in the Cleveland Clinic concluded that preoperative circulatory support, female sex and non-ischemic etiology were independent risk factors for right heart failure by multivariate analysis.[25] Researchers in Colombia University reported that a higher preoperative total bilirubin concentration was a risk factor for right heart failure.[22] These findings were compatible with those in our study.

Figure 3 is a summary of this study. As preoperative patient factors, pre-LVAS requirement for mechanical circulation with ECMO, as well as liver and renal dysfunction were independent risk factors for requiring mechanical right heart support during operation to wean off cardiopulmonary bypass. As operative factors, Toyobo device, extended cardiopulmonary bypass time and requirement for mechanical right heart support were independent risk factors for device-related infections, and left atrial drainage was an independent risk factor for post-LVAS cerebrovascular events. Additionally, higher patient age and requirement for mechanical right heart support were independent risk factors for mortality. The preoperative risk factors suggest that appropriate timing of LVAS implantation is essential for successful LVAS treatment. Establishing age-specific strategies, such as bridge to recovery[26] in young patients and destination therapy in old patients, is also important. From the operative risk factors, the development and approval for clinical use of new, small implantable devices are eagerly waited. As for the operative procedure, it is important to select an appropriate method for less invasive surgery, and to avoid using the left atrium as the inflow site. Meticulous management of right heart failure with appropriate volume control, inotropic support and nitric oxide inhalation is also required.

Study Limitations

A retrospective study and the urgent situation at the time of LVAS implantation are limitations; for example, hemodynamic variables such as right ventricular stroke work (RVSW) and the RVSW index, which have been reported as significant risk factors for right heart failure in a previous study,[21] could not be obtained in more than 25% of the present patients. Another limitation was the small numbers of each device other than the Toyobo LVAS, which limited the power to detect superiority of 1 device over another. The other limitation was that factors of postoperative management, which changed from time to time according to the accumulation of experience, were not included in the risk analysis; however, the "implanted period" may partially reflect those postoperative factors.

In conclusion, from our long-term experience with LVAS treatment at Osaka University Hospital, there is still significant mortality and morbidity after LVAS implantation. Infection and cerebrovascular events are the major limitations of long-term support. Right heart failure confers significant mortality and morbidity after LVAS implantation. As preoperative factors such as pre-LVAS mechanical circulatory support, liver and renal function are predictors for right

heart failure, appropriate selection of patients and timing of LVAS implantation are important to reduce the risk of right heart failure. Appropriate device selection, and a simple and less invasive operation may also improve the outcomes of LVAS treatment. Although risk analyses of LVAS treatment have been reported from many institutions, this study is unique because it was conducted in the situation of heart transplantation being rarely available, and the duration of LVAS support was as long as that of destination therapy.

References

1. Deng MC, Edwards LB, Hertz MI, Rowe AW, Keck BM, Kormos R, et al. Mechanical circulatory support device database of the International Society for Heart and Lung Transplantation: Third annual report, 2005. *J Heart Lung Transplant* 2005; **24:** 1182–1187.
2. Rose E, Gelijns A, Moskowitz A, Heitjan DF, Stevenson LW, Dembitsky W, et al. Long-term mechanical left ventricular assistance for end-stage heart failure. *N Engl J Med* 2001; **345:** 1435–1443.
3. Jurmann MJ, Weng Y, Drews T, Pasic M, Hennig E, Hetzer R. Permanent mechanical circulatory support in patients of advanced age. *Eur J Cardiothorac Surg* 2004; **25:** 610–618.
4. Deng MC, Loebe M, El-Banayosy A, Gronda E, Jansen PGM, Vigano M, et al. Mechanical circulatory support for advanced heart failure: Effect of patient selection on outcome. *Circulation* 2001; **103:** 231–237.
5. El-Banayosy A, Arusoglu L, Kizner L, Tenderich G, Boethig D, Minami K, et al. Predictors of survival in patients bridged to transplantation with the Thoratec VAD device: A single-center retrospective study on more than 100 patients. *J Heart Lung Transplant* 2000; **19:** 964–968.
6. El-Banayosy A, Körfer R, Arusoglu L, Kizner L, Morshuis M, Milting H, et al. Device and patient management in a bridge-to-transplant setting. *Ann Thorac Surg* 2001; **71:** S98–S102.
7. Lima B, Kherani AR, Hata JA, Cheema FH, Casher J, Oz MC, et al. Does a pre-left ventricular assist device screening score predict long-term transplantation success? A 2-center analysis. *Heart Surg Forum* 2006; **9:** E783–E785.
8. Takatani S, Matsuda H, Hanatani A, Nojiri C, Yamazaki K, Motomura T, et al. Mechanical circulatory support device (MCSD) in Japan: Current status and future directions. *J Artif Organs* 2005; **8:** 13–27.
9. Fukushima N, Miyamoto Y, Ohtake S, Sawa Y, Takahashi T, Nishimura M. Early result of heart transplantation in Japan: Osaka University experience. *Asian Cardiovasc Thorac Ann* 2004; **12:** 154–158.
10. Saito S, Matsumiya G, Sakaguchi T, Fujita T, Kuratani T, Ichikawa H, et al. Fifteen-year experience with Toyobo paracorporeal left ventricular assist system. *J Artif Organs* 2009; **12:** 27–34.
11. Matsumiya G, Saito S, Sawa Y. Extracorporeal assist circulation for heart failure. *Circ J* 2009; **73**(Suppl A): A-42–A-47.
12. Farrar DJ, Hill JD. Univentricular and biventricular Thoratec VAD support as a bridge to transplantation. *Ann Thorac Surg* 1993; **55:** 276–282.
13. Matsumiya G, Miyamoto Y, Fukushima N, Monta O, Sawa Y, Matsuda H. Intraabdominal placement of a Novacor ventricular assist system by using an expanded polytetrafluoroethylene pouch. *Ann Thorac Surg* 2004; **77:** 1851–1853.
14. Frazier OH, Myers TJ, Gregoric ID, Khan T, Delgado R, Croitoru M, et al. Initial clinical experience with the Jarvik 2000 implantable axial-flow left ventricular assist system. *Circulation* 2002; **105:** 2855–2860.
15. Samuels LE, Holmes EC, Hagan K, Gopalan R, Droogan C, Ferdinand F. The Thoratec implantable ventricular assist device (IVAD): Initial clinical experience. *Heart Surg Forum* 2006; **9:** E690–E692.
16. Siegenthaler MP, Pernice JMK, Doenst T, Sorg S, Trummer G, Friesewinkel O, et al. The Jarvik 2000 is associated with less infections than the HeartMate left ventricular assist device. *Eur J Cardiothorac Surg* 2003; **23:** 748–755.
17. Holman WL, Park SJ, Long JW, Weinberg A, Gupta L, Tierney AR, et al. Infection in permanent circulatory support: Experience from the REMATCH trial. *J Heart Lung Transplant* 2004; **23:** 1359–1365.
18. Poston RS, Husain S, Sorce D, Stanford E, Kusne S, Wagener M, et al. LVAD bloodstream infections: Therapeutic rationale for transplantation after LVAD infection. *J Heart Lung Transplant* 2003; **22:** 914–921.
19. Simon D, Fischer S, Grossman A, Downer C, Hota B, Heroux A, et al. Left ventricular assist device-related infection: Treatment and outcome. *Clin Infect Dis* 2005; **40:** 1108–1115.
20. Tsukui H, Abla A, Teuteberg JJ, McNamara DM, Mathier MA, Cadaret LM, et al. Cerebrovascular accidents in patients with a ventricular assist device. *J Thorac Cardiovasc Surg* 2007; **134:** 114–123.
21. Fukamachi K, McCarthy PM, Smedira NG, Vargo RL, Starling RC, Young JB. Preoperative risk factors for right ventricular failure after implantable left ventricular assist device insertion. *Ann Thorac Surg* 1999; **68:** 2181–2184.
22. Kavarana MN, Pessin-Minsley MS, Urtecho J, Catanese KA, Flannery M, Oz MC, et al. Right ventricular dysfunction and organ failure in left ventricular assist device recipients: A continuing problem. *Ann Thorac Surg* 2002; **73:** 745–750.
23. Morgan JA, John R, Lee BJ, Oz MC, Naka Y. Is severe right ventricular failure in left ventricular assist device recipients a risk factor for unsuccessful bridging to transplant and post-transplant mortality. *Ann Thorac Surg* 2004; **77:** 859–863.
24. Dang NC, Topkara VK, Mercando M, Kay J, Kruger KH, Aboodi MS, et al. Right heart failure after left ventricular assist device implantation in patients with chronic congestive heart failure. *J Heart Lung Transplant* 2006; **25:** 1–6.
25. Ochiai Y, McCarthy PM, Smedira NG, Banbury MK, Navia JL, Feng J, et al. Predictors of severe right ventricular failure after implantable left ventricular assist device insertion: Analysis of 245 patients. *Circulation* 2002; **106:** I-198–I-202.
26. Matsumiya G, Saito S, Sakata Y, Sawa Y. Myocardial recovery by mechanical unloading with left ventricular assist system. *Circ J* 2009; **73:** 1386–1392.